Spatial patterns of ectoenzymatic kinetics in relation to biogeochemical properties in the Mediterranean Sea and the concentration of the fluorogenic substrate used.

France Van Wambeke[1], Elvira Pulido[1], Philippe Catala[3], Julie Dinasquet[2,3], Kahina Djaoudi[1,4], Anja Engel[5], Marc Garel[1], Sophie Guasco[1], Barbara Marie[3], Sandra Nunige[1], Vincent Taillandier[6], Birthe Zäncker[6,7], Christian Tamburini[1].

[1]Aix-Marseille Université, CNRS/INSU, Université de Toulon, IRD, Mediterranean Institute of Oceanography (MIO) UM 110, 13288, Marseille, France
[2]Marine Biology Research Division, Scripps Institution of Oceanography, UCSD, La Jolla, USA
[3]Sorbonne Universités, UPMC University Paris 6, Laboratoire d'Océanographie Microbienne (LOMIC), Observatoire Océanologique, 66650, Banyuls/mer
[4]Molecular and Cellular Biology, The University of Arizona, Tucson, USA
[5]GEOMAR – Helmholtz-Centre for Ocean Research, Kiel, Germany
[6]CNRS, Sorbonne Universités, Laboratoire d'Océanographie de Villefranche (LOV), UMR7093, 06230 Villefranche-sur-Mer, France
[7]The Marine Biological Association of the UK, Plymouth, United Kingdom

Correspondence to: F. Van Wambeke (france.van-wambeke@mio.osupytheas.fr)

Abstract. Ectoenzymatic activity, prokaryotic heterotrophic abundances and production were determined in the Mediterranean Sea. Sampling was carried out in the sub surface, the deep chlorophyll maximum layer (DCM), the core of the Levantine Intermediate waters and in the deeper part of the mesopelagic layers. Michaelis-Menten kinetics were assessed, using a large range of concentrations of fluorogenic substrates (0.025 to 50 µM). As a consequence, Km and Vm parameters were determined for both low and high affinity enzymes for alkaline phosphatase, aminopeptidase (LAP) and β−glucosidase (βGLU). Based on the constant derived from the high LAP affinity enzyme (0.025-1 µM substrate concentration range), *in-situ* hydrolysis of N-protein contributed 48% ± 30% to the heterotrophic bacterial nitrogen demand within the epipelagic layers and 180% ± 154% in the Levantine Intermediate waters and the upper part of the mesopelagic layers. The LAP hydrolysis rate was higher than bacterial N demand only within the deeper layer, and only when considering the high affinity enzyme. Based on a 10% bacterial growth efficiency, the cumulative hydrolysis rates of C-proteins and C-polysaccharides contributed on average 2.5% ± 1.3 % to the heterotrophic bacterial carbon demand in the epipelagic layers sampled (sub surface and DCM). This study clearly reveals potential biases in current and past interpretations of the kinetic parameters for the 3 enzymes tested based on the fluorogenic substrates concentration used. In particular, the LAP/βGLU enzymatic ratios, and some of the depth-related trends, differed between the use of high or low concentrations of fluorogenic substrates.

1 Introduction

In aquatic environments, the organic matter compounds available for bacterial utilization are dominated by polymeric material (Simon et al., 2002; Aluwihare et al., 1997). In order to be assimilated, first they need to be hydrolyzed into smaller molecules by ectoenzymes. This represents a limiting step in organic matter degradation, and in nutrient regeneration (Hoppe, 1983; Chróst, 1991). Whether the ectoenzymatic activity should be considered as limiting the rate of organic matter remineralization is a subject of debate since hydrolysis and consumption of the by-products of hydrolysis are not always coupled (Smith et al., 1992). Bacterial ectoenzymatic hydrolysis is usually determined using fluorogenic substrates (Hoppe, 1983) which, when cleaved

Supprimé: derived from a
Supprimé: of concentrations
Supprimé: of
Supprimé: of
Supprimé: below
Supprimé: (
Supprimé:)
Supprimé: to the heterotrophic bacterial demand, by
Supprimé: for
Supprimé: dcm
Supprimé: of
Supprimé: ir
Supprimé: sets
Supprimé: aminopeptidase/βglucosidase
Supprimé: the

by the ectoenzyme, triggers the release of a fluorescent by-product. The fluorescence increase is monitored over time, thus allowing the determination of the hydrolysis rate. Kinetic experiments are time-consuming and most studies reporting ectoenzymatic activity examined enzyme kinetic patterns using one or two samples. A single presumably saturating substrate concentration is then used to determine the activity of all the samples. Baltar et al. (2009b) cite 17 published studies on ectoenzymatic activity from which 12 used a single substrate concentration, ranging from 0.02 to 1000 µM (with a median of 50 µM). Only 5 studies used a range of substrate concentrations to determine enzyme kinetics. In these 5 studies the lowest substrate concentration used was 50 nM (typically the lower concentration in the set is between 1 and 5 µM), while the highest concentration was 1200 µM (range of the higher concentrations in the set 5 - 1200 µM, with a median of 200 µM). Another compilation of data from the Mediterranean Sea (Zaccone and Caruso; 2019) showed that 6 out of 22 studies used a single concentration (assumed to be saturating) with a median of 125 µM for Leucine 7-amido 4-methyl coumarin and 50 µM for Methylumbellyferyl-phosphate. Likewise, the remaining studies assessed enzyme kinetics with a highly variable range of substrate concentrations (lowest concentrations 0.025-200 µM with a median of 0.1 µM, highest concentrations 1- 4000 µM with a median of 20 µM). However, the combination of: i) non-specificity in the enzymes, ii) the heterogeneity of enzymatic systems within single species, iii) the diversity in species present and iv) the range and variability in concentrations of surrounding substrates, will result in multiphasic kinetics (Chróst, 1991; Arnosti, 2011; Sinsabaugh and Follstad Shah, 2012 and references therein). Ectoenzymes are produced by a diversity of microorganisms. Their activity depends on a patchy distribution of natural substrates and a variety of natural (potentially unknown) molecules which can be hydrolyzed by the same enzymes, with potentially different affinities. For instance, cell-specific activities and types of activities were shown to be very variable among 44 heterotrophic bacterial strains isolated from the Californian coast and experimental phytoplankton blooms, both from particles and in the suspended phase (Martinez et al., 1996). Arrieta and Herndl (2001) showed differences in Km and Vm in an assessment of the diversity of marine bacterial β-glucosidases taken from a natural community. In the water column different kinetic systems were also observed which were generally attributed to attached or free-living bacteria having different affinities for substrates: k-strategists-oligotrophic bacteria (with both low Km and Vm) or r-strategists/copiotrophic bacteria (with both high Km and Vm, Koch, 2001). At depth, the combination of refractory DOM with recent and freshly sinking particles would promote multiphasic kinetic for ectoenzymatic activity. Biphasic kinetic systems have been described in areas where increasing gradients of polymeric material are expected due to the high concentration of particles; e.g. near the bottom and sediments for aminopeptidase (Tholosan et al., 1999), and in a shallow bay for phosphatases (Bogé et al., 2013). Most studies have shown that cell-specific ectoenzymatic activities on aggregates are ~10 fold higher than those of the surrounding assemblages (for example during a decaying bloom, Martinez et al., 1996). Biphasic kinetics were also attributed to free-living bacteria versus attached heterotrophic bacteria, the latter adapted to high substrate concentrations (with both higher Vm and Km; Unanue et al., 1999). Size fractionation is commonly carried out prior to incubation with fluorogenic substrate in order to determine in which size fraction the activity is dominant. However, size fractionation prior to incubation biases ectoenzymatic activities, due to filtration artifacts and the disruption of trophic relationships between primary producers, heterotrophic bacteria, protozoans and particulate matter. Despite such biases, carbon budgets have shown that the prokaryotes attached to aggregates are a likely source of by-products for free-living prokaryotes (Smith et al., 1992). Measurements in bulk samples enable different enzymatic kinetics to be determined without disturbing relationships between free/attached prokaryotes and DOM/POM interactions during the incubations.

Supprimé: Further,
Supprimé: a table with
Supprimé: I
Supprimé: varying
Supprimé: the
Supprimé: Of
Supprimé: ,
Supprimé: that hydrolyze the added fluorochrome
Supprimé: attached
Supprimé: assessed
Supprimé: , separated using capillary electrophoresis zymography, and showed that they had different Km and Vm
Supprimé: a
Supprimé: cope with
Supprimé: 1998
Supprimé: s
Supprimé: s

In the Mediterranean Sea, elemental C/N/P ratios of dissolved nutrients and organic matter are the subject of particular interest to elucidate the impact of P-deficiency on DOC accumulation in surface waters (Thingstad and Rassoulzadegan, 1995; Krom et al., 2004) given that the export of organic carbon in dissolved *vs.* particulate forms is linked to the P-limitation in surface layers (Guyennon et al., 2015). Since the epipelagic layers are P or N-P limited during most of the stratification period, ectoenzymes such as phosphatase and aminopeptidase providing P and N sources from organic matter have been intensively studied as indicators of these limitations (Sala et al., 2001; Van Wambeke et al., 2002). However, the potential bias introduced by multiple kinetics when comparing different types of ectoenzymes and using variable range of substrates is still poorly understood.

In this study, we investigated the Michaelis-Menten kinetics of three series of enzymes targeting proteins, phospho-mono esters and carbohydrates (leucine aminopeptidase, alkaline phosphatase and β-D –glucosidase, respectively) in the Mediterranean Sea. A wide range of substrate concentrations was tested to evaluate potential multiphasic kinetics. Our aim was to evaluate potential biases in the interpretation of past and current enzymatic kinetics based on studies measuring rates with a reduced range of substrate concentration or with the use of too high substrate concentrations. We also studied the links between ectoenzyme activities with the spatial (vertical and horizontal) trends in the quality of the available organic matter. In the Mediterranean Sea, the distribution of biogeochemical properties below the productive zone is the result of large-scale dynamic transport systems associated with three distinct thermohaline circulation cells (Wust, 1961; Hopkins, 1978; The Mermex Group, 2011 and references therein). These open cells convey fresh and cool waters of Atlantic origin to the upper 150-200 m water layer extending into the eastern part of the Levantine Sea. The return branch is composed of warm, saline waters, the Levantine intermediate waters (LIW), which spreads over the whole Mediterranean Sea at depths of 200-500 m (Kress et al., 2003; Malanotte-Rizzoli et al., 2003; Schroeder et al., 2020). In addition, two closed cells, within each Mediterranean sub-basin, are driven by deep water convection and spread below the LIW (e.g., Lascaratos et al., 1999; Testor et al., 2018).

This study focuses on the open waters of the Mediterranean Sea, examining four water layers: surface (generally P or N limited in stratification period), the deep chlorophyll maximum layer (coinciding with nutricline depths), the LIW and the deep waters. Alongside marine biogeochemical fluxes, atmospheric fluxes were quantified simultaneously during the same cruise. As a result of these exceptional simultaneous measurements, the data used in this manuscript are also used in another article of this special issue (Van Wambeke et al., 2020) where biogeochemical fluxes within the mixed layers are compared to wet and dry N and P atmospheric fluxes.

2. Materials and Methods

2.1 Sampling strategy

The PEACETIME cruise (doi.org/10.17600/15000900) was conducted from May to June 2017, along a transect extending from the Western Mediterranean Basin to the center of the Ionian Sea (25°S 115 E – 15°S, 149°W, Fig. 1). For details on the cruise strategy, see Guieu et al. (2020). Stations of short duration (< 8 h, 15 stations named SD1 to SD10, Fig. 1) and long duration (5 days, 3 stations named TYR, ION and FAST) were sampled. At least 3 casts were conducted at each short station. One focused on the first 250 m and the second one on the whole water column. These 2 casts were sampled with a standard, CTD rosette equipped with 24 Niskin bottles (12 L), and a Sea-

Supprimé: fact

Supprimé: internal

Supprimé: to

Supprimé: of fluxes on the same cruise

Supprimé: Generally, a

Bird SBE9 underwater unit equipped with pressure, temperature (SBE3), conductivity (SBE4), chlorophyll fluorescence (Chelsea Acquatracka) and oxygen (SBE43) sensors. The third cast (from surface to bottom) was carried out using a trace metal clean (TMC) rosette mounted on a Kevlar cable and equipped with Go-Flo bottles that were sampled in a dedicated trace metal free-container. The long stations situated in the center of the Tyrrhenian Sea (TYR), in the center of the Ionian Sea (ION) and in the western Algerian Basin (FAST) were selected using satellite imagery, altimetry and Lagrangian diagnostics to target dust deposition events (Guieu et al., 2020). At these stations, repeated casts were performed, alternating CTD- and TMC- rosettes.

The water sampled with the conventional CTD-rosette was used for measurements of heterotrophic bacterial production (BP, *sensus stricto* referring to heterotrophic prokaryotic production), heterotrophic bacterial abundances (BA, *sensus stricto* referring to heterotrophic prokaryotic abundances), ectoenzymatic activities (EEA), chlorophyll stocks, particulate organic carbon (POC), nitrogen (PON), phosphorus (POP) and dissolved organic carbon (DOC). Dissolved inorganic nitrogen (DIN) and phosphorus (DIP), dissolved organic nitrogen (DON) and phosphorus (DOP) were measured in samples collected using the TMC-rosette

Details on sampling and analysis for the additional parameters presented in this paper (hydrographic properties, total chlorophyll a (Tchl-a) are available in Taillandier et al. (2020), Guieu et al. (2020), and Marañón et al. (2020), in this issue.

We focused on 4 layers of the water column: two in epipelagic waters: at 5 m near the surface (SURF) and in the deep chlorophyll maximum layer (DCM) localized by the *in vivo* fluorescence measured continuously during downcasts, and two in deeper layers: in the LIW characterized by a sub-surface salinity maximum and oxygen minimum during downcasts (LIW), and at 1000 m, the limit between meso and bathypelagic waters, (MDW), except at FAST and ION, where the MDW samples were collected at 2500 m and 3000 m, respectively (Table 1).

2.2 Biochemistry

Nitrate (NO3), nitrite (NO2), and orthophosphate (DIP) concentrations were determined using a segmented flow auto-analyzer (AAIII HR Seal Analytical) according to Aminot and Kérouel (2007). The detection limits were 0.05 µM for NO3, 0.01 µM for NO2 and 0.02 µM for DIP. DON and DOP were determined after high-temperature (120 °C) persulfate wet oxidation (Raimbault et al., 1999) as follows: water sample was filtered through a 0.2 µm PES membrane and collected into 25 ml glass flasks. Samples were immediately poisoned with 100 µl H_2SO_4 5N and stored in the dark until analysis in the laboratory. Samples (20 mL) were then transferred in Teflon vials for wet oxidation. Nitrate and phosphate formed corresponding to the total N and P in the dissolved pool (TDN and TDP) were determined as described for dissolved inorganic nutrients. DON and DOP were obtained from the difference between TDN and DIN, and TDP and DIP, respectively. The limits of detection were 0.5 and 0.02 µM for DON and DOP, respectively.

Particulate organic nitrogen and phosphate (PON, POP) were determined using the same wet oxidation method (Raimbault et al., 1999). Samples (1.2 L) were collected into polycarbonate bottles and filtered through pre-combusted (450 °C, 4 h) glass fiber filters (Whatman 47mm GF/F). Filters were stored at -20°C until analysis. In the laboratory, samples were placed in Teflon vials with 20 mL of ultrapure water (Milli-Q grade) and 2.5 mL of the wet oxidation reagent for mineralization. The nitrate and orthophosphate produced were analyzed as described previously. The limits of detection were 0.02 and 0.001 µM for PON and POP, respectively.

Supprimé: the
Supprimé: data
Supprimé: :
Supprimé: localized
Supprimé: named
Supprimé: (
Supprimé: named
Supprimé: 2 stations :
Supprimé: , 2500 m
Supprimé: , 3000 m
Supprimé: abbreviated as
Supprimé: mineralization
Supprimé: Filtered s
Supprimé: and
Supprimé: n
Supprimé: i
Supprimé: where they
Supprimé: quantification

In epipelagic samples from nutrient-depleted layers, DIP and NO3 were determined using the liquid waveguide capillary cell method (LWCC) (Zhang and Chi, 2002) with enhanced sensitivity of the spectrophotometric measurement by an increase in the length of the optical path of the measurement cell to 2.5 m. For DIP, the detection limit was 0.8 nM and the response was linear up to about 150 nM, for NO3, the detection limit was 9 nM. Phospacline and nitracline depths were determined as the layers where 50 nM concentration is reached.

Samples for dissolved organic carbon (DOC) were filtered through two pre-combusted (24 h, 450°C) glass fiber filters (Whatman GF/F, 25 mm) using a custom-made glass/Teflon filtration syringe system. Samples (10 mL in duplicates) were collected into pre-combusted glass ampoules and acidified to pH 2 with phosphoric acid (H_3PO_4). Ampoules were immediately sealed and stored in the dark at room temperature. Samples were analyzed by high temperature catalytic oxidation (HTCO) on a Shimadzu TOC-V-CSH analyzer (Cauwet, 1999). Prior to injection, DOC samples were purged with CO_2 -free air for 6 min to remove inorganic carbon. 100 µL of samples were injected in triplicate and the analytical precision was 2%. Consensus reference materials (http://www.rsmas.miami.edu/groups/biogeochem/CRM.html) were injected every 12 to 17 samples to insure stable operating conditions. The nominal and measured DOC concentrations of the two batches used in this study were 42-45 µM and 43-45 µM, respectively, for batch14-2014#07-14, and 42-45 µM and 42-49 µM, respectively, for batch17-2017 #04-17. Particulate organic carbon (POC) was measured using a CHN analyzer using the improved analysis proposed by Sharp (1974).

Samples (20 ml) for total hydrolysable carbohydrates (TCHO) > 1 kDa were collected into precombusted glass vials (8 h at 500°C) and stored at -20°C until analysis. Samples were desalinated using membrane dialysis (1 kDa MWCO, Spectra Por) at 1°C for 5 h. Samples were then hydrolyzed for 20 h at 100°C with 0.8 M HCl final concentration with subsequent neutralization using acid evaporation (N_2, for 5 h at 50°C). TCHO was analyzed using high performance anion exchange chromatography with pulsed amperometric detection (HPAEC-PAD) which was applied on a Dionex ICS 3000 ion chromatography system (Engel and Händel, 2011). Two replicates for each TCHO sample were analyzed.

Total hydrolysable amino acids (TAA) were determined from 5 mL water sample collected into precombusted glass vials (8 h, 500°C) and stored at -20°C. Samples were measured in duplicates. The samples were hydrolyzed at 100°C for 20 h with 1 mL 30% HCl (Suprapur®, Merck) per 1 mL of sample and neutralized by acid evaporation under vacuum at 60°C in a microwave. Samples were analyzed using high performance liquid chromatography (HPLC) on an Agilent 1260 HPLC system following a modified version of established methods (Lindroth and Mopper, 1979; Dittmar et al., 2009). Prior to the separation of 13 amino acids with a C^{18} column (Phenomenex Kinetex, 2.6 µm, 150 x 4.6 mm), in-line derivatization with o-phthaldialdehyde and mercaptoethanol was carried out. A gradient with solvent A containing 5 % acetonitrile (LiChrosolv, Merck, HPLC gradient grade) in sodiumdihydrogenphosphate buffer (Suprapur®, Merck, pH 7.0) and acetonitrile as solvent B was used for analysis. A gradient from 100 % solvent A to 78 % solvent A was produced in 50 min.

2.3 Bacterial production

BP was determined onboard using the ^{3}H- leucine (^{3}H-Leu) incorporation technique (Kirchman, 1993) and the microcentrifuge method (Smith and Azam, 1992) for epipelagic water samples. The filtration technique was used for deep water samples as the centrifuge technique (limited to incubation volumes of 1.5 mL) is not sensitive for deep water communities. For SURF and DCM

Supprimé: the
Supprimé: whereby
Supprimé: the
Supprimé: was improved
Supprimé: g
Supprimé: s
Supprimé: lowered to
Supprimé: s
Supprimé: lowered to
Supprimé: storen
Supprimé:
Supprimé: sparged
Supprimé:) buffer (
Supprimé: (Smith and Azam, 1992)
Supprimé: ,
Supprimé: and t
Supprimé: ;
Supprimé: is
Supprimé: and

layers, triplicate 1.5 mL samples and a control killed with trichloracetic acid (TCA, 5 % final concentration) were incubated with a mixture of [4,5-^{3}H]-leucine (Amersham, specific activity 112 Ci mmol^{-1}) and nonradioactive leucine at final concentrations of 7 and 13 nM, respectively. Samples were incubated in the dark at the respective *in situ* temperatures for 1- 4 h. On 9 occasions during the cruise transect, we checked that the incorporation of leucine was linear with time. Incubations were ended by the addition of TCA to a final concentration of 5 %, followed by three runs of centrifugation at 16000 g for 10 minutes. Bovine serum albumin (BSA, Sigma, 100 mg L^{-1} final concentration) was added before the first centrifugation. After discarding the supernatant, 1.5 mL of 5 % TCA was added before the second centrifugation, and after discarding the supernatant, 1.5 mL of 80 % ethanol was added. After the third centrifugation, the ethanol supernatant was then discarded and 1.5 mL of liquid scintillation cocktail (Packard Ultimagold MV) was added. For the LIW and MDW layers, 40 mL samples were incubated in the dark for up to 12 hours at *in situ* temperature (triplicate live samples and one control fixed with 2% formalin), with 10 nM [4,5-^{3}H]-leucine. After filtration of the sample through 0.2 µm polycarbonate filters, 5% final concentration TCA was added for 10 minutes, subsequently the filter was rinsed with 10 mL 5% TCA and a final rinse with 80% ethanol.

For both types of samples (centrifuge tubes and filters) the incorporated radioactivity was counted using a Packard LS 1600 Liquid Scintillation Counter on board the ship. A factor of 1.5 kg C mol leucine^{-1} was used to convert leucine incorporation to carbon, assuming no isotopic dilution (Kirchman, 1993), as checked 4 times using concentration kinetics. Standard deviations from triplicate measurements averaged 8 % and 25 % for BP values, estimated with the centrifugation (surface layers) or the filtration technique (deep layers), respectively.

2.4 Ectoenzymatic activities

EEA were measured fluorometrically, using the following fluorogenic model substrates: L-leucine-7-amido-4-methyl-coumarin (Leu-MCA), 4 methylumbelliferyl – phosphate (MUF-P), 4 methylumbelliferyl – βD-glucopyranoside (MUF-βglu) to track aminopeptidase activity (LAP), alkaline phosphatase activity (AP), and β–glucosidase activity (βGLU), respectively (Hoppe, 1983). Stock solutions (5 mM) were prepared in methycellosolve and stored at −20°C. The amounts of MCA and MUF products released by LAP, AP and βGLU activities after addition of substrate concentrations ranging from 0.025 to 50 µM, were followed by measuring the increase in fluorescence (excitation/emission wavelength 380/440 nm for MCA and 365/450 nm for MUF, wavelength width 5 nm) in a VARIOSCAN LUX microplate reader. The instrument was calibrated with standards of MCA and MUF solutions diluted in filtered (< 0.2 µm) boiled seawater. For measurements, 2 mL of unfiltered seawater samples were supplemented with 100 µL of a fluorogenic substrate solution in a black 24-well polystyrene plate in duplicate. Incubations were carried out in the dark in thermostatically controlled incubators at *in situ* temperatures. Incubations lasted up to 24 h, with fluorescence measurements every 1 to 3 h, depending on the expected activities. The enzyme hydrolysis rate (V) was calculated from the linear part of the fluorescence versus time relationship. Boiled-water blanks were run to check for abiotic activity. The parameters Vm (maximum hydrolysis velocity) and Km (Michaelis-Menten half-saturation constant which reflects enzyme affinity for the substrate) were estimated by fitting the Michaelis-Menten function ($V = Vm \times S/(Km + S)$), to the hydrolysis rate (V) as a function of the fluorogenic substrate concentration (S) using non linear regression (PRISM4, Graph Pad software, San Diego, USA). Vm and Km were determined using 3 series of substrate concentrations: Vm_{all} and Km_{all} (global model)

Supprimé: then

Supprimé: using

Supprimé: occasional

Supprimé: em

Supprimé: Three plates were filled per layer and analyzed with the different substrates MUF-P, MCA-leu and MUF-βglu.

Supprimé: non-linear regression of

Supprimé: :

Supprimé: (

Supprimé: We determined

were calculated using a range of 11 concentrations (0.025, 0.05, 0.1, 0.25, 0.5, 1, 2.5, 5, 10, 25 and 50 µM) in duplicate, Vm_1 and Km_1 (model 1) were calculated using a restricted substrate concentration set (0.025, 0.05, 0.1, 0.25, 0.5, 1 µM) in duplicate, and Vm_{50} and Km_{50} (model 50) were calculated using the concentration set restricted to the high values of substrate (2.5, 5, 10, 25, 50 µM). The tunovertime was estimated as the ratio Km/Vm (Wright and Hobbie, 1966). We used the term 'ectoenzyme' for all types of enzymes found outside the cell, including enzymes attached on external membranes, within the periplasmic space, or free-dissolved enzymes, to broadly encompasses all enzymes located outside of intact cells regardless of the process by which such enzymes interact with the substrate.

We used an approach similar to Hoppe et al. (1993) to compute *in situ* hydrolysis rates for LAP and βGLU using total carbohydrates (TCHO) and total aminoacids (TAA) concentrations in water samples as representative of dissolved carbohydrates and proteins, respectively. The calculation for AP is presented in a companion paper from this issue (Pulido-Villena et al., in prep). These rates were calculated based on both Vm_1 and Km_1, and on Vm_{all} and Km_{all}. *In situ* hydrolysis rates expressed in nmol substrate L^{-1} h^{-1} were converted into carbon and nitrogen units using C/TCHO, C/TAA and N/TAA molar ratios.

2.5 Statistics

To assess biphasic ectoenzymatic activities, all kinetics where the coefficient of variation (standard error/mean ratio) of Vm or Km was greater than 100% were rejected. For the remaining data we used the F-test of Fisher-Snedecor as developed in Tholosan et al. (1999) to ascertain whether 2 additional parameters (Vm_1, km_1 and Vm_{50}, Km_{50} instead of Vm_{all} and Km_{all}) improved the model significantly based on the following series of equations:

$$\text{Cost (Vm, Km)} = \sum [(Vdata - Vfit)/w]^2$$

where Vdata is the experimental hydrolysis rate, Vfit the corresponding value of the fitted function, w a weighting factor set to 1, as in Tholosan et al (1999). The cost function was determined for the global model fitted with the entire set of concentrations ($cost_{all}$), model 1 ($cost_1$), and model 50 ($cost_{50}$) as:

$$\text{Var (additional parameters)} = (cost_{all} - cost_1 - cost_{50}) / 2$$

$$\text{Var (biphasic)} = (cost_1 + cost_{50}) / (n - 4)$$

Where n is the number of concentrations data in the entire data set. These 2 variances where finally compared using the F test:

$$F_{(2,\ n-4)} = \text{var (additional parameters)/var (biphasic)}$$

When the F test showed that the variances were significantly different at a probability of 0.1 we assumed that the biphasic mode was meaningful enough to explain the kinetics of the entire data set.

Trends with depth were estimated using a depth variation factor (DVF) estimated as the mean of pooled SURF and DCM data divided by the mean of pooled LIW and MDW data. This decrease (or increase), was considered as significant after a t-test comparing both series of data. The type of t test used depended on the result of a preliminary F-test checking for variance. Coefficient of variation (CV) was calculated as: standard deviation/mean x 100. Correlations among variables

Supprimé: up to 1 µM

Supprimé: or

Supprimé:)

Supprimé: entered the environment

Supprimé: (the calculation for AP is presented in a companion paper from this issue by Pulido-Villena et al., in prep),

Supprimé: on one hand

Supprimé: , for the other

Supprimé: then

Supprimé: trends within

Supprimé: firstly, we rejected

Supprimé: kinetics

Supprimé: , secondly,

Supprimé: sigma

Supprimé: like assumed

Supprimé: the

Supprimé: with low concentrations

Supprimé: the

Supprimé: with large concentrations

were examined after log transformation of the data. All mean ratios cited in the text were computed from means of ratios and not from the ratio of means.

3. Results

3.1 Physical properties

The physical properties at the sampled stations (Fig. 2), show pronounced longitudinal variation in agreement with the thermohaline circulation features of the Mediterranean Sea (see Introduction). The deep waters, formed by two separate internal convection cells, have distinct properties in the Eastern basin (station ION, temperature 13.43°C, salinity 38.73) and the Western basin (the remaining stations, temperature 12.91°C, salinity 38.48). The deep samples MDW were collected within or in the upper limits of deep waters (Fig. 2). The intermediate layer samples LIW were collected in the vicinity of the salinity maxima (Fig.2), which is used to identify the LIW core (e.g., Wust, 1961). Salinity maxima in the LIW core are particularly pronounced in the west due to the presence of fresher and lighter waters of Atlantic origin above, this feature is progressively relaxed eastward. LIW properties decrease from ION, the closest station from their source, to the westernmost stations of the Algerian Basin (ST 10, FAST), concurrent with their westward spread and progressive dilution. During the springtime expedition PEACTIME, the productive layer was stratified with the development of a seasonal thermocline. This interface separated the warm surface waters from the cool waters of Atlantic origin in which the DCM developed. As a consequence the two sample types collected in the productive layer (SURF and DCM, Fig. 2), have similar salinity, but different temperature. For the sake of clarity, the stations are presented according to their longitudinal positions, from west to east in the following order: ST10, FAST, ST1, ST2, ST3, ST4, ST5, TYR, ST6 and ION.

3.2 Biogeochemical properties

Nitrate and phosphate were depleted in the surface layers, with concentrations below the detection limits of classical methods (0.01 µM, Table S1). However, using the LWCC technique which allows to measure nanomolar variations of nutrients, DIP could be detected (Table S1) and ranged between 4 and 17 nM at 5 m depth (Table S1). Phosphaclines were deeper than nitraclines and deeper in the Eastern basin, particularly at ST 6 and ION. Chlorophyll standing stocks ranged from 18.7 to 35 mg Tchl-a m^{-2} at ST 6 and ST1, respectively (integrations down to 250 m, Table 1). The depth of the DCM ranged from 49 to 83 m depth in the Western basin, exhibiting the deepest value in the Ionian Sea (105 m depth at ION) while no obvious trend has been observed in the Tyrrhenian Sea.

DOC ranged from 39 to 75 µM (Table S1). Highest DOC values were generally observed in the surface layers and decreased by approximately 10 µM in each consecutive layer sampled. The DOC depth variation factor ranged from x1.2 to x1.6. DON ranged from 2.5 to 10.4 µM. The DON depth variation factor (DVF) was close to that of DOC (x1.2 to x1.8). DOP ranged from below our detection limit to 0.09 µM. The mean value for the DOC/DON and DOC/DOP molar ratios from all water layers were 14 ± 2 and 2112 ± 1644, respectively, with no significant change of these ratios between epipelagic layers (SURF and DCM) and deeper layers (LIW and MDW), due to the variability between stations. Deep DOP was not sampled at 3 stations. DOP estimate is subject to large errors at depth (DIP is on average 10 times higher than DOP).

Supprimé: of ‘
Supprimé: ’
Supprimé: (Vm_{all}/Vm_1, Km_{all}/Km_1, DVF, Km/Vm, DOC/DOP, DOC/DON, TAA/DON, TCHO/DOC… a
Supprimé: which is
Supprimé: other
Supprimé: layer
Supprimé: top
Supprimé: grey dots,
Supprimé: red dots,
Supprimé: s
Supprimé: which is
Supprimé: ing
Supprimé: In this
Supprimé: period
Supprimé: apparition
Supprimé: with
Supprimé: in blue dots
Supprimé: in green dots
Supprimé: their thermohaline properties
Supprimé: in
Supprimé: clearly
Supprimé: iated in
Supprimé: ranked
Supprimé: with respect to these
Supprimé: variations
Supprimé: U
Supprimé: however,
Supprimé: detected
Supprimé: to
Supprimé: Tchl*a*
Mis en forme : Police :Non Italique
Supprimé: s
Supprimé: aking all the 4 water layers, t
Supprimé: layers compared to
Supprimé: layers
Supprimé: We observed a DOC/DOP increase at the 2 deep layers sampled at 4 stations, a decrease at 2, and no trend at another.

The mean values of TAA were similar in the SURF and DCM layers, around 210 nM (Table S1, Fig. S1a) and then decreased in deep layers (LIW and MDW, $p < 0.001$). The mean DVF of TAA (x3.4) was twice as high as that of DON (x1.5) and as a consequence to, TAA-N to DON ratio (Fig. S1a) decreased significantly ($p < 0.001$) in the deep layers compared to the epipelagic layers (Fig S1a). TCHO ranged from 111 to 950 nM and the contribution of TCHO-C to DOC from 1.3 to 9.7% (Fig. S1b). At 6 stations out of 10, a minimum TCHO value was obtained in the LIW (Fig. S1b). The TCHO-C to TAA-C ratio increased significantly in the deep layers compared to the epipelagic layers ($p < 0.02$) and exhibited particularly high ratios within the Tyrrhenian sea MDW layer (ST5: 48, TYR: 24, ST6: 27).

3.3 Ectoenzymatic activities – kinetic trends

Examples of different types of kinetics are shown in Fig. 3. In general, the hydrolysis of LAP and βGLU did not completely saturate at 50 µM substrate concentration but started to reach the asymptotic value Vm. The hydrolysis rate of AP reached a maximum around 1 µM MUF-P. In this example, significant fits to Michaelis-Menten kinetic were obtained using all three models. However, significant Michaelis-Menten kinetics were also obtained regardless of the upper limit in the substrate concentration span used for the fit (Fig. S2 a, b, c). The Vm and Km characterizing these kinetics increased with the highest concentration included in the set, reaching a plateau towards the set with the largest span (more rapidly for AP, Fig. S2 c and f). In order to check for the presence of biphasic kinetic, and the effect of choosing two extreme sets of concentrations ranges, to determine EEA kinetic parameters we used systematically the 3 models described in section 2.4. The set of model 1 in the lower range of substrate concentration represents a compromise between having a sufficient set of substrate concentrations and significant enzymatic rates detected. Some kinetics were discarded i) due to the detection limits at low concentration of substrates (it was the case for all the βGLU estimates in LIW and MDW layers, Table S2), ii) due to a significant deviation from the model (in particular, when the rates did not increase between 2.5 and 50 µM substrate concentration, leading to abnormally low values of Km_{50}. This occurred in particular for AP with only 25 kinetics over 40 showing significant Michaelis-Menten kinetic estimates of the model based on high concentrations of substrates (see AP model 50, Table S2).

For LAP and βGLU, Vm_{all} and Vm_{50} were close, the distribution of these data fitted to the 1:1 axis (Fig. 4). For LAP and AP, Vm_{50} were subjected to higher errors than those of their corresponding Vm_{all} (Fig. 4), as the percentage of standard error (se%; Table S2) of Vm50 was higher than that of Vm1 in most cases (40/40 for LAP, 24/25 for AP). At the opposite, for βGLU se% was higher only in 6 out of 20 cases. The relationships between Km_{50} and Km_{all} showed the same trend, although Km_{50} were generally slightly higher than their corresponding Km_{all}, in particular for βGLU. As noted for Vm, the se% was higher for Km_{50} than for Km_1 in most of the cases for LAP (39/40) and AP (25/25) and the opposite was seen for βGLU (5/20). The standard errors of Km were higher than those of their corresponding Vm (Table S2). For LAP and βGLU, Vm_1 was notably lower than Vm_{50} and Vm_{all}; Km_1 was notably lower than Km_{50} and Km_{all}. For AP, the difference between Vm_1 and Vm_{50} was not such evident, Vm_1 being closer to Vm_{50}. However, Km_{50} was generally still much higher than Km_1.

The biphasic mode itself explained the kinetics of the entire data set in 17 cases out of 40 for LAP, in 18 cases out of 20 for βGLU and in18 cases out of 24 for AP (Table S2). Thus, the biphasic mode was enough on average to explain 60 % of the cases, with the highest proportions for βGLU. We estimated the degree of difference between the two kinetics using the 'biphasic indicator'

Supprimé: stable between
Supprimé: .
Supprimé: At all stations TAA
Supprimé: decreased from the 2 layers sampled in the epipelagic layers
Supprimé: compared to the 2 other deeper layers
Supprimé:) sampled (
Supprimé: 2
Supprimé: 2
Supprimé: with
Supprimé: layer
Supprimé: at
Supprimé: 2
Supprimé: 2
Supprimé: D
Supprimé: were obtained (see examples
Supprimé:)
Supprimé: the substrate concentration of
Supprimé: of
Supprimé: and t
Supprimé: stabilized
Supprimé: either the model 1, the model 50 or the global
Supprimé: highest pair of values (concentration, rate) included in
Supprimé: according
Supprimé: model
Supprimé: but tended to
Supprimé: to focus on
Supprimé: the
Supprimé: were then
Supprimé: determined using the model 50 (Vm_{50}, Km_{50}), the model 1 (Km_1, Vm_1) or the global model (Km_{all}, Vm_{all})
Supprimé: Our choice to use
Supprimé: corresponds to
Supprimé: in the lowest range with
Supprimé: of detection of some rates, ...
Supprimé: were
Supprimé: ing
Supprimé: addition of
Supprimé: was noted
Supprimé: as
Supprimé: were significant
Supprimé: Note however that the ...
Supprimé: (Fig. 4, Table S2)
Mis en forme : Indice
Mis en forme : Indice
Supprimé: and in
Supprimé: greatest

developed in Tholosan et al. (1999). This index tracks the difference between the initial slopes (Vm/Km) of Michaelis-Menten kinetics as (Vm_1/Km_1) / (Vm_{50}/Km_{50}). The biphasic indicator was particularly marked for βGLU (means of 87 in SURF and 47 in DCM layers), but it was highly variable (Table S2). For LAP the mean index increased from ~9 in SURF and DCM layers to ~16 within LIW and MDW layers however due to the varability of the indicator (Table S2) this increase was insignificant. For AP the biphasic indicator remained constant ($p > 0.05$) between epipelagic layers (means 12 in SURF and 6 in the DCM) and deeper layers sampled (mean of 5 in LIW and 9 in the MDW, respectively, with overall lower variability than for the 2 other enzymes, Table S2).

As the constants Km and Vm provided by the global model were very close to those of model 50; as the standard errors were mostly higher for model 50; and as the biphasic mode was not observed in all samples, we present here the kinetic parameters for the global model and model 1 (Figs. 5, 6, 7 and Table 2). Moreover, the lowest concentration range is closer to natural substrate concentrations.

For each enzyme (LAP, βGLU, AP) and the 2 models (model 1, global model), Vm was in the same order of magnitude at the SURF and DCM layers (Figs 5, 6, 7). In all layers, the highest mean Vm was obtained for AP, followed by LAP and then βGLU, independent of the model used (Table 2).

For LAP (Fig. 5), Vm_{all} was on average 3 times higher than Vm_1 in both SURF and DCM layers, but the differences between these two rates increased with depth (x8 in LIW, x12 in MDW layers). Vm_{all} decreased from epipelagic to mesopelagic layers by a factor of x8 on average, while Vm_1 decreased by a factor x19 (Fig. 5a). However, the decrease was more prominent at stations ST10 to ST5 in the Western Basin, while in Tyrrhenian waters (ST5, TYR and ST6) Vm_{all} did not show such a marked decrease with depth. The average Km_{all}/Km_1 ratio for LAP was 132. Km_{all} of LAP showed variable patterns with depth. Within the LIW and MDW layers, Km_{all} were in the same order of magnitude as in the surface, sometimes even higher (FAST, ST 3, ST5, ST6, ION) particularly in Tyrrhenian and Ionian seas (Fig. 5b). Km_1 decreased with depth in the Western stations (ST10 to ST3) whereas for stations 4, 6 and ION Km_1 was in the same order of magnitude at all depths.

For the LIW and MDW layers βGLU kinetic could not be assesses since increase of fluorescence versus time was found only for the higher substrate concentrations used. The means of βGLU rates measurable at depth were 0.010 ± 0.006 nmol L^{-1} h^{-1} in the LIW layer and 0.008 ± 0.006 nmol L^{-1} h^{-1} in the MDW layer (Fig. 6, Table 2). In the epipelagic layers (Fig. 6), Vm_{all} was on average 7 and 5 times higher than Vm_1 in SURF and DCM layers, respectively. The ratio Vm_{all}/Vm_1 was greater than those observed at the same layers for LAP or AP (Fig. 6a). The average Km_{all}/Km_1 ratio for βGLU was 311. While Km_{all} was in the same order of magnitude or slightly lower in the DCM compared to the SURF layers, the opposite trend was observed for Km_1 which tended to be higher within the DCM layer (Fig. 6b). Among the 3 ectoenzymes, βGLU showed the lowest longitudinal variability within surface layers (the longitudinal coefficient of variation (CV) was 34% for Vm_{all}, 45% for Vm_1).

AP was the enzyme for which Vm_1 and Vm_{all} were the closest (average of Vm_{all}/Vm_1 ratio for the whole data set was 1.9 ± 1.2) (Fig. 4c, 7a). Fits to model 50, using 2.5 to 50 µM concentration sets were often not significant (Table S2), because the rates stayed constant when adding these concentrations. AP within SURF layer showed pronounced relative longitudinal variability, with longitudinal CV close to 100% for Vm_{all} and Vm_1 (Table 2). Within the SURF layers AP increased towards the east, from a range of 0.5-0.9 nmol L^{-1} h^{-1} for Vm_{all} at ST10 and FAST up to 8 nmol L^{-1}

Supprimé: 68 …7 in SURF and 29 …

Supprimé: the

Supprimé: ,…and

Supprimé: s

Supprimé: systematically

Supprimé: using the…or model 50;

Supprimé: .

Supprimé: This will allow do discuss then the biases introduced by choosing a low (0.025-1 µM) set of concentration compared to a set reaching much higher concentration (here up to 50 µM) generally used by scientists making enzymatic kinetics (see the first part of the discussion)

Supprimé: each …he 2 models (mode

Supprimé:

Supprimé: the order of magnitude reached for

Supprimé: 4,

Supprimé: of the 10 studied stations

Supprimé: DVF…of x8 on average,

Supprimé: computation of □GLU

Supprimé: , confirming that saturation rates occurred with 1 µM MUF-P addition (…Figs. 3, S2) …and explained why f…

Supprimé: a larger range

h^{-1} at ION. Both AP Vm_1 and Vm_{all} decreased with depth (Fig. 7a), although both AP Vm_{all} and AP Vm_1 could be higher within the DCM layer than in the SURF layer (ST1, 2, 5 TYR, ION). At all stations Vm in the MDW were equal or lower to those in the LIW, DVF was large, varying from x1.8 to x71 for Vm_{all}, with lower values at ST10 (x1.8) FAST (x3.2) and ST3 (x 2.4), and highest DVF at ST1 (x34), ST2 (x71) and ION (x54). AP Km_{all} was on average 6 times higher than Km_1, Km_{all} increased more with depth (DVF > 0 at 8 stations and ranging from x1.4 to x19) than Km_1 (DVF > 0 at 9 stations and ranging x1.9 to x3.8, see ST1 and ST5). However, these differences between AP Km_1 and AP Km_{all} were still the lowest compared to the two other enzymes.

The turnover time of ectoenzymes (Km/Vm ratio) drives the activity at low concentrations of substrates. The incidence of the tested set of substrate concentration is very important on this parameter, as turnover times are systematically lower for the 0.025-1 µM concentration set (Table 3). The turnover times were the shortest for AP and the longest for βGLU.

3.4 Specific activities

Bulk heterotrophic prokaryotic production (BP) was of the same order of magnitude within SURF and DCM layers (Fig. S3, Table 2) and decreased towards deeper layers (DVF 59 ± 23). BA varied less than ectoenzyme Vm or BP longitudinally. Further, the decrease of BA with depth was less pronounced (DVF 7 ± 2) than BP. Cell specific BP (cs-BP) ranged from 1 to 136 x 10^{-18} g C $cell^{-1}$ h^{-1} (Table 4), decreasing with depth at all stations (DVF ranged from x4 to x23). For enzymes and BP (Fig. 8, Fig. 9, Table 2), the trend of specific activities was highly variable, with the highest DVF (decrease with depth) observed for cs-BP or cs-AP.

For LAP, specific activities ranged from 0.1 - 2.1 x 10^{-18} to 0.7 - 8 x 10^{-18} mol leu $cell^{-1}$ h^{-1}, based on Vm_1 and Vm_{all} rates, respectively (Fig. 8 a, b; Table 4 for Vm_1). A significant decrease with depth from epipelagic waters to deep waters was only found for cs-Vm_1 LAP, but not for cs-Vm_{all} LAP ($p < 0.001$, Fig 9a). While cell specific LAP Vm_1 decreased with depth, the LAP Vm_1 per unit BP increased with depth at all stations (Table 4, Fig. 9a).

For AP, specific activities ranged from 0.11 to 32 x 10^{-18} mol P $cell^{-1}$ $h^{-1}$and from 0.14 to 39 x 10^{-18} mol P $cell^{-1}$ h^{-1} based on Vm_1 and Vm_{all} rates, respectively, not differing significantly due to the small differences between AP Vm_1 and AP Vm_{all} (Fig. 8 c, d). Cs-AP exhibited either an increase (DVF < 1) or a decrease (DVF >1) with depth (Fig. 9b). AP Vm_1 per unit BP decreased with depth at all stations except at ION, whereas AP Vm_1 per unit cell increased in 7 cases over 10.

3.5 In situ hydrolysis rates

The *in situ* hydrolysis rates of TAA by LAP were higher: about ~3 times in epipelagic and about ~7 times in deep waters with the model 1 constants as compared to the global model (Fig. 10). Km_{all} were much higher than TAA concentrations (26 to 300-fold depending on the layers, Table 2, Table S1). This difference was also the case for Km_1, but the ratio between Km_1 and TAA differed by factor of 2 to 3 depending on depth layer. Consequently, *in situ* TAA hydrolysis rates by LAP based on global model represented a small percentage of Vm_{all} (highest means of 11 % in the DCM and minimum mean value 0.6 % in the MDW). However, *in situ* rates based on model 1 represented a higher proportion of Vm_1 (means 30 to 39 % depending on the layer).

The *in situ* hydrolysis rates of TCHO by βGLU were higher by ~2.5 fold using model 1 than using global model, in epipelagic layers (Fig. 11). Km_{all} were higher than *in situ* TCHO concentrations (Table 2, Table S1), by a factor ~ 18 within SURF and 22 within the DCM. Consequently, *in situ*

Supprimé: sometimes …oth AP Vm_{all} …

Commentaire [F1]: an you please explain were this this concept comes from (reference?). I understand the term turnover number (but to estimate it you also need to know the enzyme concentration).

RESPONSE : See our response in comments to the editor

Supprimé: was determined as the …

Supprimé: Both BP and BA were used to compute specific activities (Table 2, Fig S3). …ulk heterotrophic prokaryotic …

Supprimé: S

Supprimé: exhibiting a …

Supprimé: per cell…or cs-AP per cel …

Supprimé: per bacterial cell

Supprimé: obtained

Supprimé: cell-specific…s- …m_1 LAP …

Supprimé: per cell-…pecific activities …

Supprimé: using Vm_1 and Km_1 constants than using Km_{all} and Vm_{all}

Supprimé: ,

Supprimé: means ranged …6 to 300- …

Supprimé: k

Supprimé: maximal means per layer were…ighest means of 11 % in the DCM …

Supprimé: n

Supprimé: relatively …igher proportio …

Supprimé: Vm_1 and Km_1 …

Mis en forme : Police :Italique

Supprimé: about …y a factor ~ 18 …

βGLU hydrolysis rates based on global model were quasi proportional to the turnover rate Vm_1/Km_1 and represented a mean of 7% of the Vm_{all} in epipelagic layers. Km_1 were much lower than in situ TCHO concentrations (by about ~ 31 times in SURF, 8 times at the DCM) and thus most *in situ* rates based on model 1 were close to Vm_1 (93% in SURF, 79% at the DCM).

4. Discussion

4.1 The use of a broader set of substrate concentrations changes our interpretation of ectoenzymes kinetics

The idea that ectoenzyme kinetics are not monophasic is neither new nor surprising (Sinsabaugh and Follstad Shah, 2012 and references therein). However, despite the 'sea of gradients' encountered by marine bacteria (Stocker, 2012), multiphasic kinetics are seldom considered. In this work, we attempt to compare different concentration sets of fluorogenic substrates in order to evaluate the consequences on the estimated kinetic parameters in relation to the *in situ* natural concentrations of the substrates. In the coastal, epipelagic waters of the Mediterranean Sea, Unanue et al. (1999) used a set of concentrations ranging from 1 nM to 500 µM to reveal biphasic kinetics with a switch between the two phases at around 10 µM for LAP and 1-25 µM for βGLU. They referred to 'low affinity' enzymes' and 'high affinity' enzymes. In the Toulon Bay (NW Mediterranean Sea), Bogé et al. (2012) used a MUF-P range from 0.03 to 30 µM and described biphasic AP kinetics, with a switch between the 2 enzymatic systems around 0.4 µM. In our study, the biphastic indicator $(Km_{50}/Vm_{50}) / (Km_1/Vm_1)$ was used to determine the degree of difference between the two Michaelis-Menten LAP kinetics. The differences between the two LAP enzymatic systems in the water column increased with depth and could be as large as that found in sediment (biphasic indicator 20, Tholosan et al., 1999), in which large gradients of organic matter concentrations are found. However, this was not the case for all enzymes: for AP, the differences were small and consistent with depth gradients. The differences between the high and low affinity enzyme was greater for βGLU.

By comparing model 1, model 50 and the global model, and from the analysis presented in Fig S2, it is clear that the choice of the highest concentration used in the Michaelis-Menten kinetic is crucial. We decided thus not to focus our discussion on the presence or not of biphasic kinetics. Rather, we compared the effects of choosing a set of concentrations ranges sufficiently low to obtain measurable rates but at the same time encompassing the natural range of substrates (model 1 representing the high affinity system). We discuss the enzymatic properties obtained with the global model, which refers better the concentration generally used in the literature but also reflected a low affinity system compared to model 1.

Enzymatic kinetic parameters are also relevant for the interpretation of the hydrolysis of the substrate in terms of quality and quantity. For instance, the LAP Km_{all} is much higher than βGLU Km_{all} probably because LAP is not selected for low concentration ranges, in contrast to βGLU (Christian and Karl, 1995) and AP. It is also possible, however, that when the fluorogenic substrates are in the same concentration range as the natural substrates, this leads to a competition for the active sites. We can surmise that Km_1 values, although lower than published values, are still potentially overestimated. Another difference in the response to the tested range of concentrations for each substrate is the Km/Vm ratio; lower ratio indicates the adaptation to hydrolyze substrates at low concentrations. This should be considered carefully when comparing reported values.

Supprimé: Km_{all} and Vm_{all}

Supprimé: At the opposite,

Supprimé: Km_1 and Vm_1

Supprimé: ly

Supprimé: and this indicator increased with depth

Supprimé: observed

Supprimé: reach a difference

Supprimé: about

Supprimé: relatively

Supprimé: Finally, t

Supprimé: to

Supprimé: , setting the higher concentration to 50 µM

Supprimé: reflects

Supprimé: and

Supprimé: . In addition the comparison between kinetic parameters from model 1 and model 50 shows that it

Supprimé: Ratios of e

Supprimé: information

Supprimé: largely

Supprimé: adapted

Supprimé: to face

Supprimé: have

Supprimé: used by the enzyme of interest

Supprimé: thus assumed

Supprimé: ,

Supprimé: was

Supprimé: turnover time (

Supprimé:)

Supprimé: the

Supprimé: the Km/Vm, the better

We have shown that the differences between the Km and Vm of the low and high affinity enzymes might change with the nature of the enzyme, with depth, and regionally. We will develop the different interpretation emerging from i) the increase/decrease with depth ii) the use of enzymatic ratio as indicators of nutrient availability or DOM quality and iii) the estimates of *in situ* hydrolysis rates and their contribution to heterotrophic bacterial carbon or nitrogen demand.

4.2 How the set of concentration used affects ectoenzymatic kinetic trends with depth: possible links with access to particles

As shown by this study, depending on the range of concentrations tested, different conclusions can be drawn regarding increase or at least maintenance of specific levels of activity within deep layers (Koike and Nagata, 1997; Hoppe and Ulrich, 1999; Baltar et al., 2009b). Many factors, such as the freshness of the suspended particles, particle fluxes, a recent convection event, lateral advection, as well as the seasonality and taxonomic composition of phytoplankton could influence dynamics at depth, particularly in the mesopelagic layers (Tamburini et al. 2002; 2009; Azzaro et al., 2012; Caruso et al 2013; Severin et al. 2016).

AP was the enzyme that showed the smallest contrasts between different kinetics. In this study, the use of MUF-P concentrations ranging between 0.025 and 50 µM highlighted that AP rates are well described with the Michaelis-Menten Kinetic model 1, with saturation reached around 1 µM. We thus assumed that this AP activity should belong to free-living bacteria and/or dissolved enzymes (< 0.2 µm fraction) adapted to low substrate concentrations. These results agree with DOP concentrations measured, ranging between 12 and 122 nM in epipelagic waters (Pulido-Villena et al., this issue, in prep) and, when detectable, between 20 and 51 nM in deep layers. Using fractionation-filtration procedures, it has been shown that more than 50 % of the AP activity could be measured in the < 0.2 µm size fraction (Baltar, 2018 and references therein), whereas the dissolved fraction of other enzymes is generally lower. Hoppe and Ulrich (1999) found a contribution by the < 0.2 µm fraction of 41% for AP, 22 % for LAP and only 10 % for βGLU. During the PEACETIME cruise we ran a few size fractionation experiments in SURF and DCM samples (results not shown). The contribution of the < 0.2 µm fraction to the bulk activity was on average 60 ± 34 % (n = 12) for AP, 25 ± 16 % (n = 12) for βGLU and 41 ± 16 % (n = 12) for LAP, confirming these trends in the Mediterranean Sea.

Increasing AP activities per cell with depth has been reported in the Indian Ocean (down to 3000 m-depth; Hoppe and Ullrich,1999), in the subtropical Atlantic Ocean (down to 4500 m-depth; Baltar et al., 2009b) and in the central Pacific Ocean (down to 4000 m-depth; Koike and Nagata,1997). These authors used high concentrations of MUF-P (150 to 1200 µM) that could stimulate ectoenzymes of cells attached on suspended or sinking particles, and thus adapted to higher concentration ranges. However, these trends were also obtained using low concentrations (max 5 µM MUF-P), at depths down to 3500 m in the Tyrrhenian Sea (Tamburini et al., 2009). In the bathypelagic layers of the central Pacific, AP rates were up to half those observed in the epipelagic layer but the fraction < 0.2 µm was not included in the AP measurements (Koike and Nagata, 1997). These authors suggested that the deep-sea AP activity is related to fragmentation and dissolution of rapidly sinking particles. Indeed, it has been shown that the ratios of AP activity determined on particles to the AP activities in bulk seawater were highest among different tested enzymes (Smith et al., 1992). Note, however, that our study sampled only the top of mesopelagic layers (1000 m). Tamburini et al. (2002) obtained a different relative contribution of deep-sea samples when using MUF-P concentrations of 25 nM or 5 µM at the DYFAMED station in the NW

Supprimé: We have shown that
Supprimé: the debate on
Supprimé: ing
Supprimé: from the margins
Supprimé: both
Supprimé: fit
Supprimé: t
Supprimé: with affinities
Supprimé: average
Commentaire [F2]: I am surprised by this statement: The DOP values shown in Table S1 are similar everywhere and in all layers and around 50-40nM

Response : these are ranges, not means
Supprimé: ~ 40
Supprimé:
Supprimé: of
Supprimé: some
Supprimé: layers
Supprimé: ;
Supprimé: 250 µM, concentration kinetics from 0.6 to 1200 µM and 150 µM, respectively
Supprimé: face
Supprimé: accounted for as much
Supprimé: as
Supprimé: of
Supprimé: dissolved AP
Supprimé: due
Supprimé: concentrated
Supprimé: had the highest concentration factor compared
Supprimé: of
Supprimé: data generally
Supprimé: stops
Supprimé: in

Mediterranean Sea (down to 2000 m-depth), further showing the artefact of the concentration used. The deep enzymatic activities could be x1.4 to x2.6 times higher due to the effect of hydrostatic pressure. Specific AP decreased at 5 stations, increased in 3 other stations and at the 2 remaining stations specific Vm_{all}, increased while specific Vm_1 decreased (Fig. 9b). Similarly for the deepest layers sampled (FAST: 2500 m and ION: 3000 m), results showed also no depth trend since specific AP decreased with depth at ION and increased at FAST. The POC/POP ratio did not change with depth. However, the variability in the trend with depth seen for the specific AP activities was also observed in the DOC/DOP ratio. In short, while we expected to see an increase in specific activities with depth due to a preferential removal of P, this was not systematically the case.

LAP activities showed more pronounced trends with depth than AP. Cell-specific LAP showed contradictory results: at all stations cell-specific Vm_1 decreases with depth (according to the DVF criterion, Fig. 9a) whereas Vm_{all} remained stable (2 stations over 10) or increased with depth (5 stations over 10). Using a high concentration of MCA-leu other authors have found an increase in LAP activity per cell with depth in bathypelagic layers (Zaccone et al., 2012; Caruso et al., 2013).

The use of a large concentration set also impacts the Km values, because if only a high concentration range is used, the kinetic contribution of any enzyme with high affinity would be hidden. Baltar et al. (2009b), using a concentration of substrates ranging from 0.6 to 1200 µM, reported an increase in the Km of LAP (from ~400 to 1200 µM) and AP (from ~2 to 23 µM) with depths down to 4500 m in the sub-tropical Atlantic. In contrast, Tamburini et al. (2002), using a concentration of substrates ranging from 0.05 to 50 µM, obtained lower Km values (ranging between 0.4 and 1.1 µM) for LAP in the Mediterranean deep waters (down to 2000 m depth). It is however difficult to come to a conclusion about the effect of the concentration set tested on Km variability with depth by comparing 2 studies from different environments and using different sets of substrate concentrations. In our study where both kinetics were determined in the same waters, among the two parameters Vm and Km, Km showed the largest differences between the 2 types of kinetics. At many stations (TYR, ION, FAST and ST10), the Km_1 of LAP was stable or decreased with depth whereas Km_{all} increased, suggesting that within deep layers LAP activity was linked more to the availability of suspended particles or fresh organic matter from sinking material, than to DON. Thus, the difference between Km_1 and Km_{all} might reflect adaptative strategies to spatial and/or temporal patchiness in the distribution of suspended particles. Freshly sinking material was probably not present in our incubations, because of the small volume of water used, but could have contributed to the release of free bacteria, small suspended particles and DOM within its associated plume (Azam and Long, 2001; Tamburini et al., 2003; Grossart et al., 2007; Fang et al., 2014). Baltar et al. (2009a) also suggested that hot spots of activity at depth were associated with particles. The fact that the C/N ratio of particulate material increased with depth (from 11-12 to 22-25) but not so much for DOC/DON (from 13-12 to 14-15 from SURF and DCM to LIW and MDW, respectively) also indicates a preferential utilization of protein substrates from particles. Recently, Zhao et al. (2020) suggested that deep-sea prokaryotes and their metabolism are likely associated with particles rather than DOC, based on the increasing contribution of genes encoding secretory enzymes. In contrast to the results for AP, the higher differences between the two LAP enzymatic systems, suggest that the microorganisms responsible for the LAP activity face large gradients of protein concentrations and are adapted to pulsed inputs of particles.

4.3 How the set of concentrations used affects interpretation of enzymatic properties as indicators of nutrient imbalance of DOM quality and stoichiometry

Supprimé: Furthermore, t
Supprimé: when not in the convectiv...
Supprimé: Vm increased based on
Supprimé: but
Supprimé: based on Vm_1
Supprimé: Note that
Supprimé: are also
Supprimé: contrasting
Supprimé: decreases
Supprimé: but
Supprimé: increases
Supprimé: particulate matter
Supprimé:
Supprimé: with
Supprimé: We
Supprimé: however, it
Supprimé: enzymatic systems
Supprimé: differences
Supprimé: and different trends with ...
Supprimé: , Vm_{all} decreased with dept...
Supprimé: systematically
Supprimé: P Km
Supprimé: Km
Supprimé: Km_{all} in particular, increase...
Supprimé: LAP
Supprimé: LAP
Supprimé: it is LAP
Supprimé: which
Supprimé: greatest
Supprimé: LAP
Supprimé: LAP
Supprimé: associated to
Supprimé: y to
Supprimé: adapt
Supprimé: a potential
Supprimé: is
Supprimé: statistically not included in...
Supprimé: incubated
Supprimé: that
Supprimé: confirms
Supprimé: on the utilization of ...
Supprimé: the
Supprimé: Conversely to
Supprimé: results
Supprimé: 2
Supprimé: expressing
Supprimé: d
Supprimé: were
Supprimé: ¶

In epipelagic waters, both AP maximum rates (Vm_1, Vm_{all}) significantly increased by around 3 fold from the Algerian/Ligurian Basins to the Tyrrhenian Basin (t test, p = 0.002 and p = 0.02, respectively) and reached maximum values at ION. This longitudinal increase was also confirmed by specific activities. This increase in cell-specific AP activities appears to follow a decrease in phosphate availability. While inorganic phosphate can be assimilated directly through a high affinity absorption pathway, the assimilation of DOP requires its mineralization to free DIP which is then assimilated. POP is an indicator of living biomass and enzyme producers, but the correlation between VmAP and POP were negative in the surface layers (log-log relationship, r = - 0.86, -0.88 for Vm_{all} and Vm_1, respectively, p < 0.01 in both cases), suggesting the progressive eastward decline of living biomass and its and phosphate availability was accompanied by increased AP expression. Vm in the surface did not correlate with DIP, however the relative DIP deficiency increased eastward, suggested by the deepening of the phosphacline (Table 1), the decrease in average DIP concentrations within the phosphate-depleted layer and the decrease in P diffusive fluxes reaching the surface layer (Pulido-Villena et al. 2020, in prep, this issue). Along a trans-Mediterranean transect, Zaccone et al. (2012), did not observe a relation between DIP and AP, although they also found increased values of AP specific activities in the Eastern Mediterranean Sea. Bogé et al. (2012), using a concentration set close to ours (0.03-30 µM MUF-P) obtained biphasic kinetics with high differences in the two Vm values (contrary to our results) and described different relationships between Vm and DOP or DIP depending on the low or high affinity enzyme. Such differences could be due to the large gradient of trophic conditions in their study, carried out in an eutrophic bay where DOP and DIP concentration ranged from 0 to 185 nM, and from 0 to 329 nM, respectively. In contrast, the range of DIP concentrations in our surface water samples was narrow and values were very low (4 - 17 nM).

The AP/LAP activity ratio can be used as an indicator of N - P imbalance as demonstrated in enrichment experiments (Sala et al., 2001). In this study using high concentrations of substrates (200 µM) the authors described a decrease in the AP/LAP activity ratio following DIP addition and, conversely, a large increase (10-fold) after the addition of 1 µM nitrate. In their initial experimental conditions, the ratios ranged from 0.2 to 1.9. We observed a similar low ratio in the western Mediterranean Sea, but in the Ionian Sea the AP/LAP activity ratio reached 17 (Vm_{all}) and 43 (Vm_1, Fig. S4a), suggesting that nutrient stresses and imbalances can be as important and variable in different regions of the Mediterranean. Such imbalances are more visible in the high affinity systems.

LAP/βGLU activity ratio is used as an index of the ability of marine bacteria to preferentially metabolize proteins rather than polysaccharides. Within epipelagic layers, the prevalence of LAP over βGLU is common in temperate areas (Christian and Karl, 1995; Rath et al., 1993) and in high latitudes (Misic et al., 2002, Piontek et al., 2014). The LAP/βGLU activity ratio varied widely from the Equator to the Southern Ocean, ranging from 0.28 to 593 (Sinsabaugh and Follstad Shah, 2012). In the Ross Sea, this ratio exhibited a relationship with primary production (Misic et al., 2002). In the Caribbean Sea, along an eutrophic to oligotrophic gradient, the LAP/βGLU activity ratio increased in oligotrophic conditions (Rath et al., 1993). In the epipelagic zone, during our study, a small westward gradient in productivity (18 to 35 mg TChla m^{-2}) was found, LAP /βGLU activity ratios ranged from east to west between 3 and 17 for Vm_{all}, and from 8 to 34 for Vm_1 (Fig. S4b) and thus varied according to the productivity gradient but also to the concentration set tested, in agreement with previous reported ratios (10 and 20 for the low concentration and high concentration range, respectively; Unanue et al., 1999). Finally, the LAP/βGLU activity ratios

Supprimé: in AP activity
Supprimé: calculating
Supprimé: which also increased towards ION
Supprimé: of
Supprimé: DIP
Supprimé: DIP
Supprimé: AP
Supprimé: that POP reflected
Supprimé: increased capacity to derepress AP genes.
Supprimé: AP rates
Supprimé: trend
Supprimé: also
Supprimé: for the 2 types of kinetics
Supprimé: with
Supprimé: and
Supprimé: according to
Supprimé: and
Supprimé: s
Supprimé: which studied
Supprimé: order to circumvent the effect of depth, correlations are described in our study only for 10 surface data where the DIP concentration range is narrow
Supprimé:)
Supprimé: Sea, as observed after manipulation of nutrients. We have shown that s
Supprimé: when using a low range of concentrations
Supprimé: a recurrent observation
Supprimé: For example,
Supprimé: with values
Supprimé: -
Supprimé: toward
Supprimé: y
Supprimé: and Herndl
Supprimé: the degree of trophic conditions exhibited
Supprimé: of
Supprimé:
Supprimé: along the Western to the Eastern Mediterranean Sea. Following this gradient
Supprimé: to
Supprimé: range

reported here and other studies using low substrate ranges are lower than when using higher concentration sets: 20-200 in the subarctic Pacific (Fukuda et al., 2000, using 200 µM concentration), 213 at station ALOHA in the equatorial Pacific (Christian and Karl, 1995, using L-leucyl-β–naphtylamine instead of MCA-leu at 1000 µM and MUF-βGLU at 1.6 µM), suggesting that the LAP/βGLU activity ratio is highly variable and with a non linear dependence on the fluorogenic substrate concentration. As observed for AP/LAP, the LAP/βGLU activity ratio showed much higher variations for the low affinity enzyme.

Throughout the water column, variations in the relative activity of different enzymes is also suggested as a possible indicator of changes in bacterioplankton nutrition patterns. The LAP/βGLU activity ratio decreased with depth, following the decrease in the protein to carbohydrate ratio of particulate material (Misic et al., 2002), as nitrogen is re-mineralized faster than carbon. However, the TAA-C/TCHO-C ratios were consistently higher within the DCM layer (~90 m) than at the surface and the LAP/βGLU activity ratio of both Vm_1 and Vm_{all} increased as a consequence, revealing important DON cycling (relative to DOC) at the DCM in comparison to the mixed layers. Below the DCM, the particulate C/N ratio increased with depth and TAA-C /TCHO-C decreased, likewise indicating a faster hydrolysis of N rich compounds. We estimated Vm_{all} LAP/Vm_{all} βGLU activity ratios from a few of the single rates measured at high concentration (most βGLU kinetics at depth were not available), and observed, in contrast to Misic et al. (2002), an increase of the ratio within deep layers, as βGLU decreased faster than LAP with depth. A bias could be due to the absence of βGLU kinetics at depth, nevertheless other authors have also shown an increase of LAP/βGLU activity ratios with depth (Hoppe and Ullrich, 1999 in Indian Ocean, Placenti et al., 2018 in the Ionian Sea).

4.4 How the set of concentration used affects potential contribution of macromolecules hydrolysis to bacterial production

Our results clearly showed the influence of the concentration set used to estimate *in situ* hydrolysis rates. If the experimentally added substrate concentration is clearly above the possible range of concentrations found in the natural environment *in situ* rates could be largely overestimated. To obtain a significant determination of the *in situ* rates, the added substrate concentrations should be close to the range of variation expected in the studied environment (Tamburini et al., 2002).

We compared the *in situ* LAP hydrolysis rates to the N demand of heterotrophic prokaryotes (which was based on BP data assuming no active excretion of nitrogen and a C/N ratio of 5). Similarly, the in situ rates of TAA plus TCHO were compared to the bacterial carbon demand (based on a bacterial growth efficiency of 10% (Gazeau et al., 2021, Céa et al., 2014, Lemée et al., 2002). Using the global model, *in situ* hydrolysis of TAA by LAP contributed only 25% ± 22% of the bacterial N demand in epipelagic layers and 26% ± 24% in deep layers. This contribution increased using the high affinity enzyme constants (48% ± 29% and 180% ± 154 % in epipelagic layers and deep layers, respectively). In the North Atlantic, the contribution of LAP hydrolysis rates of particles (0.3 µM MCA-leucine added) to bacterial nitrogen demand varied between 63 and 87%, increasing at 200 m. Crottereau and Delmas (1998) computed also *in situ* hydrolysis using combined amino-acid concentrations and LAP kinetics and found a range of 6-121% contribution to bacterial N demand in aquatic eutrophic ponds. A large variability of LAP hydrolysis contribution to bacterial N demand has also been detected in coastal-estuarine environments using a radiolabeled natural protein as a substrate (2 - 44%, Keil and Kirchman, 1993). Piontek et al. (2014) used the turnover of

Supprimé: in this study
Supprimé: work
Supprimé: still
Supprimé: s
Supprimé: 1995
Supprimé: ratio
Supprimé: according to
Supprimé: and not in a regular way
Supprimé: the
Supprimé: ratio
Supprimé: exacerbated
Supprimé: o
Supprimé: when using
Supprimé: over the high affinity enzyme
Supprimé: being
Supprimé: here
Supprimé: was
Supprimé: what occurred in
Supprimé: layer
Supprimé: supporting
Supprimé: organic sources than C organic sources
Supprimé: compute
Supprimé: TAA concentrations were lower than Km_1 and Km_{all}
Supprimé: The two Michaelis–Menten plots cross each other, at a substrate value of about 1.8 ± 1.3 µM for LAP and 1.7 ± 0.6 µM for βGLU. Considering the TAA range, and the high affinity enzyme (Km_1 Vm_1) with its low Km and high turnover rates, *in situ* rates are consequently higher using the high affinity enzyme kinetics. Although TCHO ranges were lower than Km_1 but higher than Km_{all}, TCHO was always lower than the crossing concentration point of the two types of kinetics, and consequently, again, the us ...
Supprimé: bacterial production
Supprimé: biomass
Supprimé: , with no active excretion c ...
Supprimé: , and
Commentaire [F3]: again clumsy a ...
Supprimé: ,
Supprimé: this issue, in prep
Supprimé: low affinity enzyme ...
Supprimé:)
Mis en forme : Police :Italique
Supprimé: to
Supprimé: combined
Supprimé: *kinetics of*
Mis en forme : Police :Italique
Supprimé: LAP with
Supprimé: Pointek

βGLU and LAP determined with 1 µM analog substrate concentrations to compute in situ TCAA and TCHO hydrolysis rates along a 79°N transect in the North Atlantic and showed that 134% and 52% of BP could be supported by peptide and polysaccharides hydrolyzed by enzyme activities, respectively. Based on a bacterial growth efficiency of 10%, these fluxes will represent 10 times less, i.e. 13 and 5 % of bacterial carbon demand, which is in the order of magnitude that we obtained. In our study, the contribution of TAA hydrolysis to bacterial N demand was higher in the DCM than in the SURF (10 to 40% based on the high affinity enzyme). Nevertheless, this calculation may be biased as marine cyanobacteria such as *Synechococcus* and *Prochlorococcus*, which are dominating phytoplankton groups in the Mediterranean Sea (Siokou-Frangou et al., 2010), can also express LAP (Martinez and Azam, 1993) to satisfy their N requirements. During our study, primary production (PP) peaked in the DCM (Marañón et al., 2020). Size fractionation of primary production showed the importance of phytoplankton excretion, which contributed between 20 to 55% of the total PP depending on stations (Marañón et al, 2020). Within the surface mixed layer, other sources of N such as atmospheric deposition could sustain a significant part of bacterial N demand. The dry atmospheric deposition (inorganic+ organic) of N at all stations within the PEACETIME cruise corresponded to 25 ± 17% of bacterial N demand (Van Wambeke et al, 2020).

The *in situ* cumulated hydrolysis rates of TCHO by βGLU, estimated only in epipelagic layers were ~3 times higher using the high affinity enzyme. We summed C sources coming from the hydrolysis by LAP and by βGLU in epipelagic layers (Fig. 11) and compared them to the bacterial carbon demand. Dissolved proteins and combined carbohydrates contributed to only a small fraction of the bacterial carbon demand: 1.5% based on the low affinity enzyme and 3 % based on the high affinity enzyme.

Only within deeper layers the hydrolysis rates of TAA at some stations were higher than bacterial N demand, suggesting that proteolysis is one of the major sources of N for heterotrophic bacteria in aphotic layers. However, this was only based on the high affinity enzymes where we found cases of over-hydrolysis of organic nitrogen (Fig. 10). This over-hydrolysis was particularly marked in the LIW of the Tyrrhenian Basin, where over-hydrolysis up to 220% was obtained as well as higher TAA concentrations in comparison to 'older' LIW waters in the Algerian Basin. TAA decreased faster than DON along the LIW trajectory, indicating that the labile DON fraction (combined amino acids) was degraded first. Sinking particles or large aggregates associated with attached bacteria are considered to be major providers of labile organic matter for free bacteria (Smith et al., 1992). Within the 5 mL volume of water hydrolyzed for TAA analysis, and the 2 mL water volume used to determine ectoenzymatic kinetics, most of this particulate detrital pool is underrepresented, and thus the contribution of TAA hydrolysis to bacterial nitrogen demand is underestimated. However, there is an increasing evidence of release from particles not only of monomers issued from hydrolysis, but also of ectoenzymes produced by deep-sea prokaryotes attached on particles themselves (Zhao et al., 2020). This could explain why, in our small volumes, we still observe multiple kinetics. Studying alkaline phosphatase activity in the Toulon Bay, Bogé et al. (2013) observed biphasic kinetics only in the dissolved phase, which also suggests that low affinity AP originates from enzyme secretion by prokaryotes attached to particles. Further, the study of size fractionated particulate material showed that the origin of the low affinity enzymes was mostly within the > 90 µm fraction (Bogé et al., 2017).

5 Conclusions

Commentaire [F4]: Assuming an given efficiency for C assimilation is necessary either when estimating growth rates or biomass accumulation. Here, since you discuss only C uptake the values you should look at are simply BP.
RESPONSE
See our response in comments to the editor

Supprimé: is increasing

Supprimé: with

Supprimé: compared to

Supprimé: layer

Supprimé: from means of

Supprimé: This is consistent, however, as some

Supprimé: and *Synechococcus* and *Prochlorococcus* are dominant

Supprimé: phytoplankton groups in the Mediterranean Sea (Siokou-Frangou et al., 2010)

Supprimé: In

Supprimé: I

Supprimé: the DCM was an active biomass layer where

Supprimé: the

Supprimé: Likewise, t

Supprimé: It is o

Supprimé: that

Supprimé: more important

Supprimé: Vm_1 and Km_1 kinetic parameters (i.e. the

Supprimé:)

Supprimé: water mass

Supprimé: in which

Supprimé: so

Supprimé: We could consider that with t

Supprimé: this

Supprimé: of big size or big density (i.e. fast sinking particles)

Supprimé: a

Supprimé: of bulk sea water sample not representative of big or fast sinking particles

Supprimé: low affinity enzyme

Supprimé: from

Supprimé: Afterwards

Supprimé: , this team focused their research by

Supprimé: fractionation

Supprimé: of

Supprimé: and they found

Supprimé: due

Supprimé: to

Supprimé: , i.e. big particles

Vertical and regional variability in enzyme activities were found in the Mediterranean Sea, where heterotrophic prokaryotes face not only carbon, but also N and P limitations. Although biased by the use of artificial fluorogenic substrates, ectozenzymatic activity is an appropriate tool to study the adaptation of prokaryotes to the environmental gradients in stoichiometry, chemical characteristics and organic matter concentrations. We have shown that the relative increase or decrease of Vm or specific activities per depth are largely related to the choice of concentration set used in the kinetic measurements. The activity ratios of AP/LAP or LAP/βGLU used to track nutrient imbalances in the DOMpool showed larger range of variation in low affinity enzymes. Finally, to obtain robust determination of *in situ* enzymatic rates, the added substrate concentrations should be close to the range of variation expected in the studied area. While the use of microplate titration technique greatly improved the simultaneous study of different enzymes, assessments of enzyme kinetics should be performed systematically in enzymatic studies. Future combination of such techniques with the chemical identification of DOC and DON pools, and meta-omics, as well as the use of marine snow catchers, will help our understanding of the biodegradation of organic matter in the ocean.

Supprimé: of
Supprimé: shown
Supprimé: large
Supprimé: d quantities of
Supprimé: they face, especially when using high concentrations
Supprimé: debates about
Supprimé: s
Supprimé: s
Supprimé: of DOM quality changes
Supprimé: s
Supprimé: using
Supprimé: rather than large
Supprimé: a significant
Mis en forme : Police :Non Italique
Supprimé: environment
Supprimé: EEAs
Supprimé: further
Supprimé: enzymatic
Supprimé: a ‘sea of gradients’

Data availability

Data will be accessible once the special issue is published at the French INSU/CNRS LEFE CYBER database: http://www.obs-vlfr.fr/proof/php/PEACETIME/peacetime.php, last access: 29 October 2020. Scientific coordinator: Hervé Claustre; data manager, webmaster: Catherine Schmechtig. The policy of the database is detailed here: http://www.obs-vlfr.fr/proof/dataconvention.php (last access: 29 October 2020).

Supprimé: http://www.obs-vlfr.fr/proof/php/PEACETIME/peacetime.php
Supprimé: http://www.obs-vlfr.fr/proof/dataconvention.php

Author contribution

FVW and CT designed the study. FVW, CT, MG and SG sampled and incubated samples for ectoenzymatic activity on board, FVW and SG analyzed the ectoenzymatic data. FVW and MG sampled and analyzed BP samples, BZ sampled and analyzed TAA and TCHO samples, AE managed the TCHO an TAA analysis and treatments, EP and KD sampled and analyzed DIP analysis with the LWCC technique, SN sampled and analyzed nutrients and organic matter, VT assisted in CTD operations and analyzed water masses, JD sampled for DOC and flow cytometry, PC analyzed bacterial abundances, BM analyzed DOC, FVW prepared the ms with contribution from all co-authors.

Competing interests

The authors declare that they have no conflict of interest

Special issue statement

This article is part of the special issue ‘Atmospheric deposition in the low-nutrient–low-chlorophyll (LNLC) ocean: effects on marine life today and in the future (ACP/BG inter-journal SI)’. It is not associated with a conference

Financial support

This study is a contribution of the PEACETIME project (http://peacetime-project.org), a joint initiative of the MERMEX and ChArMEx components supported by CNRS-INSU, IFREMER, CEA, and Météo-France as part of the programme MISTRALS coordinated by INSU (doi:

10.17600/17000300*).* The project leading to this publication has received funding from European FEDER Fund under project 1166-39417.

Acknowledgements: The authors thank also many scientists & engineers for their assistance with sampling/analyses: J. Roa for TCHO, R. Flerus for TAA, J. Guittoneau for nutrients, T. Blasco for POC, J. Uitz and C. Dimier for Chl a (analysed at the SAPIGH HPLC analytical service at the IMEV, Villefranche), I. Obernosterer for DOC. We warmly thank C. Guieu and K. Deboeufs, as coordinators of the program PEACETIME. We are grateful to the two anonymous reviewers and the editor C. Klass for their constructive and pertinent comments.

References

Aminot, A., and Kérouel, R.: Dosage automatique des nutriments dans les eaux marines, in: Méthodes d'analyses en milieu marin, edited by: IFREMER, 188 pp, 2007.

Aluwihare, L. I., Repeta, D. J., and Chen, R. F.: A major biopolymeric component to dissolved organic carbon in surface sea water, Nature, 387, 166–169. doi : 10.1038/387166a0, 1997.

Arnosti, C.: Microbial Extracellular enzymes and the marine carbon cycle, Ann. Rev. Mar. Sci., 3, 401-425, 2011.

Arrieta, J. M., and Herndl, G. J.: Assessing the diversity of marine bacterial β-glucosidases by capillary Electrophoresis Zymography, Appl. Environ. Microb., 67, 4896–4900, 2001.

Azam, F., and Long, R. A.: Sea snow microcosms, Nature, 414, 495–498, 2001.

Azzaro, M., La Ferla, R., Maimone, G., Monticelli, L. S., Zaccone, R., and Civitarese, G.: Prokaryotic dynamics and heterotrophic metabolism in a deep convection site of Eastern Mediterranean Sea (the Southern Adriatic Pit), Cont. Shelf Res., 44, 06–118, doi: 10.1016/j.csr.2011.07.011, 2012.

Baltar, F., Arístegui, J., Gasol, J. M., Sintes, E., and Herndl, G. J.: Evidence of prokaryotic metabolism on suspended particulate organic matter in the dark waters of the subtropical North Atlantic, Limnol. Oceanogr., 54, 182–193, doi:10.4319/lo.2009.54.1.0182, 2009a.

Baltar, F., Aristegui, J., Sintes, E., van Aken, H. M., Gasol, J. M., and Herndl, G. J.: Prokaryotic extracellular enzymatic activity in relation to biomass production and respiration in the meso- and bathypelagic waters of the (sub)tropical Atlantic, Env. Microbiol., 11, 1998–2014, 2009b.

Baltar, F.: Watch Out for the "Living Dead": Cell-Free Enzymes and Their Fate, Front. Microbiol., 8, article 2438, doi: 10.3389/fmicb.2017.02438, 2018.

Bogé G., Lespilette, M., Jamet, D., and Jamet, J-L.: Role of sea water DIP and DOP in controlling bulk alkaline phosphatase activity in N.W. Mediterranean Sea (Toulon, France), Mar. Pollut. Bull., 64, 1989–1996, doi: 10.1016/j.marpolbul.2012.07.028, 2012.

Bogé, G., Lespilette, M., Jamet, D., and Jamet, J.-L.: The relationships between particulate and soluble alkaline phosphatase activities and the concentration of phosphorus dissolved in the seawater of Toulon Bay (NW Mediterranean). Mar. Pollut. Bull., 74, 413–419, doi: 10.1016/j.marpolbul.2013.06.003, 2013.

Bogé, G., Lespilette, M., Jamet, D., and Jamet, J.-L.: Role of DOP on the alkaline phosphatase activity of size fractionated plankton in coastal waters in the NW Mediterranean Sea (Toulon Bay, France), Mar. Pollut. Bull., 117, 264–273, doi:10.1016/j.marpolbul.2016.11.037, 2017.

Caruso, G., Monticelli, L., La Ferla, R., Maimone, G., Azzaro, M., Azzaro, F., Decembrini, F., De Pasquale, F., Leonardi, M., Raffa, F., Zappal, G., and De Domenico, E.: Patterns of Prokaryotic Activities and Abundance among the Epi-Meso and Bathypelagic Zones of the Southern-Central Tyrrhenian Sea, Oceanography, 1, 1, doi: 10.4172/ocn.1000105, 2013.

Cauwet, G.: Determination of dissolved organic carbon (DOC) and nitrogen (DON) by high temperature combustion, in: Methods of Seawater analysis, edited by: Grashoff, K., Kremling, K, and Ehrhard, M., 3rd Ed., Wiley-VCH, Weinheim, 407–420, 1999.

Céa, B., Lefèvre, D., Chirurgien, L., Raimbault, P., Garcia, N., Charrière, B., Grégori, G., Ghiglione, J.-F., Barani, A., Lafont, M., and Van Wambeke, F.: An annual survey of bacterial production, respiration and ectoenzyme activity in coastal NW Mediterranean waters: temperature and resource controls, Environ. Sci. Pollut. Res., doi: 10.1007/s11356-014-3500-9, 2014.

Christian, J. R., and Karl, D. M.: Bacterial ectoenzymes in marine waters: Activity ratio and temperature responses in three oceanographic provinces, Limnol. Oceanogr., 40, 1046–1053, 1995.

Chróst, R.J. Microbial enzymes in aquatic environments, Springer-Verlag, New York, 1991.

Crottereau, C., and Delmas, D.: Exoproteolytic activity in an Atlantic pond (France): estimates of in situ activity, Aquat. Microb. Ecol., 15, 217–224, 1998.

Supprimé: -

Supprimé: (2001)

Supprimé: -

Supprimé: .

Supprimé: -

Supprimé: Baklouti, M., Diaz, F., Pinazo, C., Faure, V., and Quéguiner, B.: Investigation of mechanistic formulations depicting phytoplancton dynamics for models of marine pelagic ecosystems and description of a new model, Prog. Oceanogr., 71, 1–33, doi:1016/j.pocean.2006.05.002, 2006.¶

Supprimé: -

Supprimé: -

Supprimé: -

Supprimé:

Supprimé: -

Supprimé: -

Supprimé: .

Supprimé: -

Dittmar, T.H., Cherrier, J., and Ludwichowski, K.-U: The analysis of amino acids in seawater, in: Practical Guidelines for the Analysis of Seawater, edited by: Wurl, O., Boca Raton, FL: CRC-Press, 67–78, 2009.

Engel, A., and Händel, N.: A novel protocol for determining the concentration and composition of sugars in particulate and in high molecular weight dissolved organic matter (HMW-DOM) in seawater, Mar. Chem. 127, 180–191, 2011.

Fang, J., Zhang, L., Li, J., Kato, C., Tamburini, C., Zhang, Y., Dang, H., Wang, G., and Wang, F.: The POM-DOM piezophilic microorganism continuum (PDPMC) - The role of piezophilic microorganisms in the global ocean carbon cycle, Science China (Earth Sciences), 1–10, doi:10.1007/s11430-014-4985-2, 2014.

Fukuda, R., Sohrin, Y., Saotome, N., Fukuda, H., Nagata, T., and Koike, I.: East-west gradient in ectoenzyme activity in the subartic Pacific: Possible regulation by zinc, Limnol. Oceanogr., 45, 930–939, 2000.

Gazeau, F., Van Wambeke, F., Marañón, E., Pérez-Lorenzo, M., Alliouane, S., Stolpe, C., Blasco, T., Leblond, N., Zäncker, B., Engel, A., Marie, B., Dinasquet, J., and Guieu, C.: Impact of dust addition on the metabolism of Mediterranean plankton communities under present and future conditions of pH and temperature, Biogeosciences Discuss., bg-2021-20, 2021.

Grossart, H.-P., Tang, K. W., Kiørboe, T., and Ploug, H.: Comparison of cell-specific activity between free-living and attached bacteria using isolates and natural assemblages, FEMS Microb. Lett., 266, 194–200, doi:10.1111/j.1574-6968.2006.00520.x, 2007.

Guieu, C., D'Ortenzio, F., Dulac, F., Taillandier, V., Doglioli, A., Petrenko, A., Barrillon, S., Mallet, M., Nabat, P., and Desboeufs, K.: Introduction: Process studies at the air-sea interface after atmospheric deposition in the Mediterranean Sea - objectives and strategy of the PEACETIME oceanographic campaign (May–June 2017), Biogeosciences, 17, 5563–5585, doi:10.5194/bg-17-5563-2020, 2020.

Guyennon, A., Baklouti, M., Diaz, Palmiéri, J., Beuvier, J., Lebeaupin-Brossier, C., Arsouze, T., Beranger, K., Dutay, J.-C., and Moutin, T.: New insights into the organic carbonexport in the Mediterranean Sea from 3-D modeling, Biogeosciences, 12, 7025–7046, doi: 10.5194/bg-12-7025-2015, 2015.

Hopkins, T. S.: Physical processes in the Mediterranean Basin, In: Estuarine transport processes, edited by Kjerfve, B., University of South Carolina, 269–310, 1978.

Hoppe, H.-G.: Significance of exoenzymatic activities in the ecology of brackish water: measurements by means of methylumbelliferyl-substrates, Mar. Ecol. Prog. Ser., 11, 299–308, 1983.

Hoppe, H.-G., and Ullrich, S.: Profiles of ectoenzymes in the Indian Ocean: phenomena of phosphatase activity in the mesopelagic zone, Aquat. Microb. Ecol., 19, 139–148, 1999.

Hoppe, H.-G., Ducklow, H., and Karrasch, B.: Evidence for dependency of bacterial growth on enzymatic hydrolysis of particulate organic matter in the mesopelagic ocean, Mar. Ecol. Prog. Ser,, 93, 277–283, 1993.

Keil, R.G, and Kirchman, D.:Dissolved combined amino acids: Chemical form and utilization by marine bacteria, Limnol. Oceanogr., 38: 1256–1270, 1993.

Kirchman, D. L.: Leucine incorporation as a measure of biomass production by heterotrophic bacteria, in: Handbook of methods in aquatic microbial ecology, edited by: Kemp, P.F., Sherr, B.F., Sherr, E.B. and Cole, J.J., Lewis, Boca Raton, 509–512, 1993.

Koch, A.L.: Oligotrophs versus copiotrophs, BioEssays, 23, 657–661, 2001.

Koike, I., and Nagata, T.: High potential activity of extracellular alkaline phosphatase in deep waters of the central Pacific, Deep-Sea Res. PT II, 44, 2283–2294, 1997.

Kress, N., Manca, B., Klein, B., and Deponte, D.: Continuing influence of the changed thermohaline circulation in the eastern Mediterranean on the distribution of dissolved oxygen and nutrients: Physical and chemical characterization of the water masses, J. Geophys. Res. Oceans, 108, 8109, doi:10.1029/2002JC001397, 2003.

Krom, M. D., Herut, B. and Mantoura, R. F. C.: Nutrient budget for the eastern Mediterranean: Implication for phosphorus limitation, Limnol. Oceanogr, 49, 1582–1592, doi:10.4319/lo.2004.49.5.1582, 2004.

Supprimé: .
Supprimé: I
Supprimé: .
Supprimé: &
Supprimé: —
Supprimé: -
Supprimé: enrichment
Supprimé: carbon budget and
Supprimé: in prep., this issue.
Supprimé: -
Supprimé: -
Supprimé: .
Supprimé: B.
Supprimé: editor
Supprimé: -
Supprimé: -
Supprimé: -
Supprimé: -
Supprimé: -
Supprimé: .
Supprimé: I
Supprimé: -
Supprimé: -
Supprimé: -

Lascaratos, A., Roether, W., Nittis, K., and Klein, B.: Recent changes in deep water formation and spreading in the eastern Mediterranean Sea: a review, Prog. Oceanogr., 44, 5–36, 1999.

Lemée, R., Rochelle-Newall, E., Van Wambeke, F., Pizay, M.-D., Rinaldi, P., and Gattuso, J.-P.: Seasonal variation of bacterial production, respiration and growth efficiency in the open NW Mediterranean Sea., Aquat. Microb. Ecol., 29, 227–237, 2002

Lindroth, P., and Mopper, K.: High performance liquid chromatographic determination of subpicomole amounts of amino acids by precolumn fluorescence derivatization with o-phthaldialdehyde, Anal. Chem. 51, 1667–1674, 1979

Malanotte-Rizzoli P., Manca, B.B., Marullo,S., Ribera d'Alcalà,M., Roether, W., Theocharis, A., and Conversano, F.: The Levantine Intermediate Water Experiment (LIWEX) Group: Levantine basin - A laboratory for multiple water mass formation processes, J. Geophys. Res-Oceans, 108, doi:10.1029/2002JC001643, 2003.

Marañón, E., Van Wambeke, F., Uitz, J., Boss, E.S., Pérez-Lorenzo, M., Dinasquet, J., Haëntjens, N., Dimier, C., and Taillandier, V.: Deep maxima of phytoplankton biomass, primary production and bacterial production in the Mediterranean Sea during late spring, Biogeosciences Discuss., https://doi.org/10.5194/bg-2020-261, in review, 2020.

Martinez, J., and Azam, F.: Aminopeptidase activity in marine chroococcoid cyanobacteria, Appl. Environ. Microb., 59, 3701–3707, 1993.

Martinez, J., Smith, D. C., Steward, G. F., and Azam, F.: Variability in ectohydrolytic enzyme activities of pelagic marine bacteria and its significance for substrate processing in the sea, Aquat. Microb. Ecol., 10, 223–230, 1996.

Misic, C., Povero, P., and Fabiano, M.: Ectoenzymatic ratios in relation to particulate organic matter distribution (Ross Sea, Antarctica), Microb. Ecol., 44, 224–234, doi:10.1007/s00248-002-2017-9, 2002.

Piontek, J., Sperling, M., Nothig, E.-V., and Engel, A.: Regulation of bacterioplankton activity in Fram Strait (Arctic Ocean) during early summer: The role of organic matter supply and temperature, J. Marine Syst., 132, 83–94, doi: 10.1016/j.jmarsys.2014.01.003, 2014.

Placenti, F., Azzaro, M., Artale, V., La Ferla, R., Caruso, G., Santinelli, C., Maimone, G., Monticelli, L. S., Quinci, E. M., and Sprovieri, M.: Biogeochemical patterns and microbial processes in the Eastern Mediterranean Deep Water of Ionian Sea, Hydrobiologia, 815, 97–112, doi: 10.1007/s10750-018-3554-7, 2018.

Pulido-Villena, E., Van Wambeke, F., Desboeufs, K., Petrenko, A., Barrillon, S., Djaoudi, K., Doglioli, A., D'Ortenzio, F., Fu, Y., Gaillard, T., Guasco, S., Nunige, S., Raimbault, P., Taillandier, V., Triquet, S., and Guieu, C. Analysis of external and internal sources contributing to phosphate supply to the upper waters of the Mediterranean Sea (Peacetime cruise), in prep for Biogeosciences, special issue PEACETIME.

Raimbault, P., Pouvesle W., Diaz F., Garcia N., and Sempere, R.: Wet-oxidation and automated colorimetry for simultaneous determination of organic carbon, nitrogen and phosphorus dissolved in seawater, Mar. Chem. 66, 161–169, 1999.

Rath, J., Schiller, C., and Herndl, G. J.: Ectoenzyme activity and bacterial dynamics along a trophic gradient in the Caribbean Sea, Mar. Ecol. Prog. Ser., 102, 89–96, 1993.

Sala, M. M., Karner, M., Arin, L., and Marrassé, C.: Measurement of ectoenzyme activities as an indication of inorganic nutrient imbalance in microbial communities, Aquat. Microb. Ecol., 23, 301–311, doi:10.3354/ame023301, 2001.

Severin, T., Sauret, C., Boutrif, M., Duhaut, T., Kessouri, F., Oriol, L., Caparros, J., Pujo-Pay, M., Durrieu de Madron, X., Garel, M., Tamburini, C., Conan, P., and Ghiglione, J. F.: Impact of an intense water column mixing (0–1500 m) on prokaryotic diversity and activities during an open-ocean convection event in the NW Mediterranean Sea, Environ. Microbiol., 18, 4378–4390, doi:10.1111/1462-2920.13324, 2016.

Siokou-Frangou, I., Christaki, U., Mazzocchi, M. G., Montresor, M., Ribera d'Alcala, M., Vaque, D., and Zingone, A.: Plankton in the open Mediterranean Sea: a review, Biogeosciences, 7, 1543–1586, doi:10.5194/bg-7-1543-2010, 2010.

Stocker, R.: Marine Microbes See a Sea of gradients, Science, 38, 628-633, 2012.

Supprimé: -

Supprimé: .

Supprimé: .

Supprimé: -

Supprimé: -

Supprimé: -

Supprimé: -

Code de champ modifié

Supprimé: -

Supprimé: Rath, J., and Herndl, G. J.: Characteristics and Diversity of ß-D-Glucosidase (EC 3.2.1.21) Activity in Marine Snow, Appl. Environ. Microbiol., 60, 807-813, 1994.¶

Supprimé: -

Supprimé: -

Supprimé: -

Sharp, J. H.: Improved analysis for "particulate" organic carbon and nitrogen from seawater, Limnol. Oceanogr., 19, 984–989, 1974.
Schroeder, K., Cozzi S., Belgacem, M., Borghini, M., Cantoni, C., Durante, S., Petrizzo, A., Poiana, A., and Chiggiato, J.: Along-Path Evolution of Biogeochemical and Carbonate System Properties in the Intermediate Water of the Western Mediterranean, Front. Mar. Sci., 7:375, doi: 10.3389/fmars.2020.00375, 2020.
Simon, M., Grossart, H., Schweitzer, B., and Ploug, H.: Microbial ecology of organic aggregates in aquatic ecosystems, Aquat. Microb. Ecol., 28, 175-211, doi: 10.3354/ame028175, 2002.
Sinsabaugh, R., and Follstad Shah, J.: Ectoenzymatic Stoichiometry and Ecological Theory, Annu. Rev. Ecol., Evol. S., 43, 313–343, doi:10.1146/annurev-ecolsys-071112-124414, 2012.
Smith, D. C. and Azam, F.: A simple,economical method for measuring bacterial protein synthesis rates in sea water using 3H-Leucine, Mar. Microb. Food Webs, 6, 107–114, 1992.
Smith, D. C., Simon, M., Alldredge, A. L., and Azam, F.: Intense hydrolytic activity on marine aggregates and implications for rapid particle dissolution, Nature, 359, 139–142, 1992.
Taillandier, V., Prieur, L., D'Ortenzio, F., Riberad'Alcala, M., and Pulido-Villena, E.: Profiling float observation of thermohaline staircases in the western Mediterranean Sea and impact on nutrient fluxes, Biogeosciences, 17, 3343–3366, doi: 10.5194/bg-17-3343-2020, 2020.
Tamburini, C., Garcin, J., Ragot, M., and Bianchi, A.: Biopolymer hydrolysis and bacterial production under ambient hydrostatic pressure through a 2000 m water column in the NW Mediterranean, Deep-Sea Res. PT II, 49, 2109–2123, doi:10.1016/S0967-0645(02)00030-9, 2002.
Tamburini, C., Garcin, J., and Bianchi, A.: Role of deep-sea bacteria in organic matter mineralization and adaptation to hydrostatic pressure conditions in the NW Mediterranean Sea, Aquat. Microb. Ecol., 32, 209–218. Doi: 10.3354/ame032209, 2003.
Tamburini, C., Garel, M., Al Ali, B., Mérigot, B., Kriwy, P., Charrière, B., and Budillon, G.: Distribution and activity of Bacteria and Archaea in the different water masses of the Tyrrhenian Sea, Deep Sea Res. PT II, 56, 700–714, doi: 10.1016/j.dsr2.2008.07.021, 2009.
Testor, P., Bosse, A., Houpert, L., Margirier, F., Mortier, L., Legoff, H., Dausse, D., Labaste, M., Kartensen, J., Hayes, D., Olita, A. Ribotti, A., Schroeder, K., Chiggiato, J., Onken, R., Heslop, R., Mourre, B., D'Ortenzio, F., Mayot, N., Lavigne, H., de Fommervault, O., Coppola, L., Prieur, L., Taillandier, V., Durrieu de Madron, X., Bourrin, F., Many, G., Damien, P., Estournel, C., Marsaleix, P., Taupier-Lepage, I., Raimbault, P., Waldman, R., Bouin, M-N., Giordani, H., Caniaux, G., Somot, S., Ducrocq, V. and Conan P.: Multiscale observations of deep convection in the northwestern Mediterranean Sea during winter 2012–2013 using multiple platforms, J. Geophys.Res. Oceans, 123, 1745–1776. doi:10.1002/2016JC012671, 2018.
The Mermex Group. Marine ecosystems' responses to climatic and anthropogenic forcings in the Mediterranean, Prog. Oceanogr., 91(2), 97–166, doi: 10.1016/j.pocean.2011.02.003, 2011.
Thingstad, T. F., and Rassoulzadegan, F.: Nutrient limitations, microbial food webs, and 'biological C-pumps': suggested interactions in a P-limited Mediterranean, Mar. Ecol. Prog. Ser., 117, 299–306, 1995.
Tholosan, O., Lamy, F., Garcin, J., Polychronaki, T., and Bianchi, A.: Biphasic extracellular proteolytic enzyme activity in benthic water and sediment in the North Western Mediterranean Sea, Appl. Environ. Microb., 65, 1619–1626, 1999.
Unanue, M., Ayo, B., Agis, M., Slezak, D., Herndl, G. J., and Iriberri, J.: Ectoenzymatic activity and uptake of monomers in marine bacterioplankton described by a biphasic kinetic model, Microb. Ecol., 37, 36–48, doi:10.1007/s002489900128, 1999.
Van Wambeke, F., Christaki, U., Giannakourou, A., Moutin, T., and Souvemerzoglou, K.: Longitudinal and vertical trends of bacterial limitation by phosphorus and carbon in the Mediterranean Sea, Microb. Ecol., 43, 119–133, doi: 10.1007/s00248-001-0038-4, 2002.
Van Wambeke, F., Taillandier V., Desboeufs, K., Pulido-Villena, E., Dinasquet, J., Engel, A., Marañón, E., Ridame, C., and Guieu, C.: Influence of atmospheric deposition on biogeochemical cycles in an oligotrophic ocean system, Biogeosciences Discuss., https://doi.org/10.5194/bg-2020-411, 2020.

Supprimé: -
Supprimé: (2020)
Supprimé: .
Supprimé: -
Supprimé: -
Supprimé: -
Supprimé: .
Supprimé: https://
Supprimé: .org/
Supprimé: .
Supprimé: -
Supprimé: -
Supprimé: Unanue, M., Azua, I., Arrieta, J. M., Labirua-Iturburu, A., Egea, L., and Iriberri, J.: Bacterial colonization and ectoenzymatic activity in phytoplankton-derived model particles: Cleavage of peptides and uptake of amino acids., Microb. Ecol., 35, 136-146, ,1998.¶
Supprimé: -

Wright, R. T., and Hobbie, J. E.: Use of glucose and acetate by bacteria and algae in aquatic ecosystems, Ecology, 47, 447–464, 1966.

Wust, G.: On the vertical circulation of the Mediterranean Sea, J. Geophys. Res., 66, 10, 3261-3271, 1961.

Zaccone, R., and Caruso, G.: Microbial enzymes in the Mediterranean Sea: relationship with climate changes, AIMS Microbiology, 5, 251–272, 2019.

Zaccone, R., Boldrin, A., Caruso, G., La Ferla, R., Maimone, G., Santinelli, C., and Turchetto, M.: Enzymatic Activities and Prokaryotic Abundance in Relation to Organic Matter along a West–East Mediterranean Transect (TRANSMED Cruise), Microb. Ecol., 64, 54–66, 2012.

Zhang, J.-Z., and Chi, J.:Automated analysis of nano-molar concentrations of phosphate in natural waters with liquid waveguide, Environ. Sci. Technol., 36, 1048–1053, doi:10.1021/es011094v, 2002.

Zhao, Z., Baltar, B., and Herndl, G. J.: Linking extracellular enzymes to phylogeny indicates a predominantly particle-associated lifestyle of deep-sea prokaryotes, Sciences Advances, 6, eaaz4354, https://doi.org/10.1126/sciadv.aaz4354, 2020.

Supprimé: -

Supprimé: -

Supprimé: -

Figure Legends

Figure 1. Sampling sites. Colour codes on dots correspond to the plots on Fig.2

Figure 2. T/S diagram for the sampled stations. Main water masses are MAW: Modified Atlantic Waters, LIW: Levantine intermediate Waters, WMDW: Western Mediterranean Deep waters, EMDW: Eastern Mediterranean Deep Waters.

Figure 3. Michaelis-Menten kinetics for the DCM layer at station FAST. a, b, c: data are shown by the dots, continuous lines correspond to the non linear regression of the global model (concentration set 0.025 to 50 µM) and dotted lines of model 50. d, e, f: Michaelis-Menten kinetics for model 1 (concentration set 0.025-1 µM).

Figure 4. Relationships between kinetic parameters resulting from model 1, model 50 and global model for the three ectoenzymes (a, d: Leucine aminopeptidase (LAP), b, d: βglucosidase (βGLU), c, f : alkaline phosphatase (AP). a,b,c: relationships between Vm_1 and Vm_{all} and between Vm_{50} and Vm_{all}; d,e, f: relationships between Km_1 and Km_{all} and between Km_{50} and Km_{all}; and. Error bars show standard errors. The standard error of Km_{all} in d, e, f (white dots) is not plotted for clarity.

Figure 5. Distribution of kinetic parameters Vm (a) and Km (b) for leucine aminopeptidase (LAP) calculated from model 1 (Vm_1, Km_1) and the global model (Vm_{all}, Km_{all}). Error bars represents the standard errors derived from the non linear regressions.

Figure 6. Distribution of kinetic parameters Vm (a) and Km (b) for βglucosidase (βGLU) calculated from model 1 (Vm_1, Km_1) and the global model (Vm_{all}, Km_{all}) in SURF and DCM. Error bars represents the standard errors derived from the non linear regressions. In the LIW and MDW layers kinetics were impossible to compute due to the low number of measurable rates (see results). The black bar in a) is assumed to represent a minimal value for Vm_{all}.

Figure 7. Distribution of kinetic parameters Vm (a) and Km (b) for alkaline phosphatase (AP) calculated from model 1 (Vm_1, Km_1) and the global model (Vm_{all}, Km_{all}). Error bars are the standard errors derived from the non linear regressions.

Figure 8. Box plot distributions of cell specific (cs-) Vm_1 and Vm_{all}, for leucine aminopeptidase (a, b) and alkaline phosphatase (c, d). Box limits are 25% and 75% percentiles, horizontal bar is median, red cross is mean, blue dots are outliers.

Figure 9. Depth variation factor (DVF, unitless) for enzymatic specific activities. DVF is calculated as the mean of pooled data from the SURF and DCM layers divided by the mean of pooled data from the LIW and MDW layers. a: DVF of cell-specific leucine aminopeptidase (cs-Vm_{all} and cs-Vm_1); b: DVF of cell specific alkaline phosphatase (cs- Vm_{all} and cs-Vm_1); c: For β–glucosidase DVF, cell specific activities are based on the few detectable rates at high concentration (yellow dots). Black crosses show the DVF of cell-specific heterotrophic prokaryotic production (cs-BP).

Figure 10. *In situ* hydrolysis rates of proteins (nmol N L^{-1} h^{-1}), determined from TAA and LAP ectoenzyme kinetics for the high and low affinity systems, and heterotrophic bacterial nitrogen demand, determined from BP assuming a C/N molar ratio of 5 and no active excretion of nitrogen. a) epipelagic layers (SURF, DCM), b) deeper layers (LIW, MDW).

Figure 11. *In situ* hydrolysis rates of carbohydrates and proteins (nmol C L^{-1} h^{-1}), determined from TAA, TCHO and LAP and βGLU ectoenzymatic kinetics for the low and high affinity systems, and heterotrophic bacterial carbon demand (BCD, determined from BP assuming a BGE of 10% in epipelagic waters. Note the different scale for bacterial carbon demand on the right.

Supprimé: Physical properties along the different
Supprimé: :
Supprimé: T/S diagram
Supprimé: . Colour codes correspond similar to the stations mapped Fig. 1
Supprimé: Principal …ain water mass …
Supprimé: Example of …ichaelis- …
Supprimé: in the relationships between Km_{all} and Km_1 (…n d, e, f , …
Supprimé: For all the other dots, when the error bar is not visible, it is included in the data dot.¶
Supprimé: leucine aminopeptidase (LAP
Supprimé:
Supprimé: The e…ror bars are …
Supprimé: βglucosidase (βGLU) …
Supprimé: alkaline phosphatase (AP) …
Supprimé: specific …m_1 and Vm_{all} pe…
Supprimé: decreas…ariationing…fac…
Supprimé: dissolved …roteins and …
Supprimé: dissolved and particulate detrital …arbohydrates and C-…roteins …

2020

Table 1. Characteristics of the stations. Lat: Latitude, Long: Longitude, Bott D : bottom depth, T_{5m} : Temperature at 5m depth, Ncline depth : nitracline depth, calculated as the layer where NO3 reaches 50 nM; , Pcline depth : phosphacline depth, estimated as the layer where DIP reaches 50 nM; ITchl-a: 0-250 m integrated total chlorophyll a, LIW D: depth of the LIW layer sampled, MDW D: depth of the MDW layer sampled

	sampling date	Lat °N	Long °E	Bott D m	T_{5m} °C	DCM D m	Ncline D m	Pcline D m	I Tchl -a mg m^{-2}	LIW D m	MDW D m
ST 10	6/8/2017	37.45	1.57	2770	21.6	89	30	69	28.9	500	1000
FAST	6/3/2017	37.95	2.92	2775	21.0	87	50	59	27.3	350	2500
ST 1	5/12/2017	41.89	6.33	1580	15.7	49	48	76	35.0	500	1000
ST 2	5/13/2017	40.51	6.73	2830	17.0	65	40	70	32.7	500	1000
ST 3	5/14/2017	39.13	7.68	1404	14.3	83	47	100	23.2	450	1000
ST 4	5/15/2017	37.98	7.98	2770	19.0	64	42	63	29.2	500	1000
ST 5	5/16/2017	38.95	11.02	2366	19.5	77	42	78	30.5	200	1000
TYR	5/17/2017	39.34	12.59	3395	19.6	73	82	95	31.3	200	1000
ST 6	5/22/2017	38.81	14.50	2275	20.0	75	43	113	18.7	400	1000
ION	5/25/2017	35.49	19.78	3054	20.6	105	85	231	27.7	250	3000

Supprimé: IChla

Supprimé: C

Table 2. Heterotrophic bacterial abundances (BA), bacterial production (BP) and ectoenzyme kinetic parameters of the global model (Vm_{all}, Km_{all}) obtained from the entire substrate range (0.025 to 50 µM) and model 1 (Vm_1, Km_1) obtained from the low substrate range (0.025 to 1 µM) for leucine aminopeptidase (LAP), β-glucosidase (βGLU) and alkaline phosphatase (AP) at the 4 layers. Means ± sd and range values given for all stations). Maximum velocity rates (Vm_{all} and Vm_1), half saturation constants (Km_{all} and Km_1). nk: No kinetic available as not enough significant rates to plot Michaelis-Menten kinetics.

		SURF	DCM	LIW	MDW
Vm_{all} LAP	mean ± sd	0.97 ± 0.79	1.20 ± 0.92	0.22 ± 0.18	0.15 ± 0.08
nmol l^{-1} h^{-1}	range	0.36 – 2.85	0.35 – 2.83	0.08 – 0.69	0.06 – 0.28
Vm_1 LAP	mean ± sd	0.29 ± 0.10	0.45 ± 0.25	0.028 ± 0.014	0.017 ± 0.010
nmol l^{-1} h^{-1}	range	0.21 – 0.56	0.19 – 0.98	0.014 – 0.060	0.007 – 0.042
Vm_{all} βGLU	mean ± sd	0.13 ± 0.04	0.11 ± 0.06	nk	nk
nmol l^{-1} h^{-1}	range	0.08 – 0.23	0.03 – 0.22		
Vm_1 βGLU	mean ± sd	0.019 ± 0.009	0.025 ± 0.019	nk	nk
nmol l^{-1} h^{-1}	range	0.012 – 0.040	0.014 – 0.077		
Vm_{all} AP	mean ± sd	2.52 ± 2.62	3.73 ± 4.52	0.38 ± 0.48	0.24 ± 0.40
nmol l^{-1} h^{-1}	range	0.30 – 8.30	0.11– 14.6	0.04 – 1.66	0.06 – 1.30
Vm_1 AP	mean ± sd	1.55 ± 1.58	3.01 ± 4.01	0.24 ± 0.33	0.12 ± 0.25
nmol l^{-1} h^{-1}	range	0.25 – 5.62	0.07–13.2	0.02 – 1.11	0.01 – 0.80
Km_{all} LAP	mean ± sd	6.0 ± 5.6	5.3 ± 7.6	16.4 ± 13.3	15.2 ± 11.3
µM	range	0.8 – 20.9	0.7 – 25.0	3.6 – 38.1	1.8 – 34.6
Km_1 LAP	mean ± sd	0.49 ± 0.18	0.43 ± 0.27	0.23 ± 0.19	0.13 ± 0.11
µM	range	0.12 – 0.70	0.07 – 0.90	0.10 – 0.69	0.01 – 0.39
Km_{all} βGLU	mean ± sd	10.6 ± 6.3	7.7 ± 5.1	nk	nk
µM	range	4.4 – 27.4	1.2–14.2		
Km_1 βGLU	mean ± sd	0.044 ± 0.071	0.11 ± 0.11	nk	nk
µM	range	0.009 – 0.244	0.01 – 0.36		
Km_{all} AP	mean ± sd	0.58 ± 0.67	0.49 ± 0.34	2.25 ± 2.42	2.6 ± 3.5
µM	range	0.09 – 2.18	0.18 – 1.07	0.17 – 7.32	0.4 – 11.9
Km_1 AP	mean ± sd	0.11 ± 0.03	0.27 ± 0.28	0.37 ± 0.22	0.27 ± 0.16
µM	range	0.07 – 0.14	0.05 – 0.80	0.14 – 0.89	0.06 – 0.52
BA	mean ± sd	5.3 ± 1.6	5.4 ± 1.5	1.13 ± 0.40	0.56 ± 0.15
10^5 cells ml^{-1}	range	2.1 – 7.8	4.0 – 8.5	0.41 – 1.91	0.33 – 0.78
BP	mean ± sd	37 ± 13	21 ± 7	0.77 ± 0.40	0.27 ± 0.19
ng C l^{-1} h^{-1}	range	26 – 64	12 – 32	0.39 – 1.60	0.07 – 0.60

Table 3. Turnovertimes of ectoenzymes (Km/Vm ratio). Means ± sd and range values given . For leucine aminopeptidase (LAP), beta glucosidase (βGLU), and alkaline phosphatase (AP). nd no kinetics, not enough rates to plot Michaelis Menten kinetics. The turnovertimes are calculated from the global model (Km_{all}/Vm_{all}) or the model 1 (Km_1/Vm_1). nk: No kinetic available as not enough significant rates to plot Michaelis-Menten kinetics.

	Units: days	SURF	DCM	LIW	MDW
Km_{all}/Vm_{all} LAP	mean ± sd	255 ± 79	158 ± 182	3394 ± 2629	4161 ± 1806
	range	94 – 340	40 – 663	1294 – 9016	1308 – 7028
Km_1/Vm_1 LAP	mean ± sd	74 ± 26	42 ± 22	345 ± 235	343 ± 298
	range	15 – 106	15 – 82	141 – 985	55 – 959
Km_{all}/Vm_{all} βGLU	mean ± sd	3464 ± 1576	3091 ± 1551	nk	nk
	range	1997-7395	328-5481		
Km_1/Vm_1 βGLU	mean ± sd	126 ± 233	247 ± 273	nk	nk
	range	20-784	15-873		
Km_{all}/Vm_{all} AP	mean ± sd	12 ± 9	39 ± 46	563 ± 542	914 ± 817
	range	2 – 33	0.7 – 113	16 – 1441	20 – 2719
Km_1/Vm_1 AP	mean ± sd	5.6 ± 5.0	27 ± 37	268 ± 349	301 ± 172
	range	1 – 17	0.6 – 106	12 – 1180	14 – 594

Supprimé: f
Supprimé: nk
Supprimé: c
Supprimé: k
Supprimé: ld
Supprimé: ld
Supprimé: nd
Supprimé: nd
Supprimé: ld
Supprimé: ld
Supprimé: nd
Supprimé: nd

Table 4. Range of different specific activities calculated using Vm_1 and specific to either i) abundance of total heterotrophic prokaryotes (cell specific activities, cs), ii) heterotrophic bacterial production (per bp LAP, per bp βGLU, per bp AP). DVF is the 'depth variation factor', calculated for each station as mean value in epipelagic water (SURF and DCM data) divided by the mean in deep waters (LIW and MDW). The distribution of cs-Vm_1 and cs-Vm_{all} for AP and LAP are also presented on Fig 8.

enzyme	units	SURF	DCM	LIW	MDW	*DVF*
cs-LAP	10^{-18} mol leu $bact^{-1}$ h^{-1}	0.33 – 1.52	0.44 – 2.18	0.11-0.70	0.13 – 0.54	*1.3 – 9.6*
cs-βGLU	10^{-18} mol glucose $bact^{-1}$ h^{-1}	0.02 – 0.11	0.02 – 0.17	nd	nd	*nd*
cs-AP	10^{-18} mole P $bact^{-1}$ h^{-1}	0.45 – 26	0.11 – 32	0.13-11	0.17-23	*0.1 – 28*
csBP	10^{-18}g C $bact^{-1}$ h^{-1}	46 – 136	25 – 60	3 – 17	1 – 14	*4 – 23*
per bp LAP	nmol AA nmol C^{-1}	0.04 – 0.24	0.12 – 0.44	0.21 – 1.08	0.36 – 3.03	*0.09 – 0.76*
per bp βGLU	nmol glucose nmol C^{-1}	0.003 – 0.017	0.007 – 0.034	nd	nd	*nd*
per bp AP	nmol P nmol C^{-1}	0.09 – 2.3	0.05 – 11	0.46 – 8	0.6-40	*0.04 – 1.7*

Supprimé: potential
Supprimé: per cell
Supprimé: unit BP
Supprimé: decreasing
Supprimé:
Supprimé: cell specific
Supprimé:
Supprimé: cell specific
Supprimé:
Supprimé: 7
Supprimé: Per cell
Supprimé:
Supprimé: Per cell
Supprimé:
Supprimé: Per cell
Supprimé:
Supprimé: Per cell
Supprimé:
Supprimé: BP
Supprimé: BP
Supprimé: BP

Spatial patterns of ectoenzymatic kinetics in relation to biogeochemical properties in the Mediterranean Sea and the concentration of the fluorogenic substrate used.

France Van Wambeke, Elvira Pulido, Philippe Catala, Julie Dinasquet, Kahina Djaoudi, Anja Engel, Marc Garel, Sophie Guasco, Barbara Marie, Sandra Nunige, Vincent Taillandier, Birthe Zäncker, Christian Tamburini,

Supplementary Material

Figure S1. a) Distribution of total aminoacids (TAA, bars, lef scale) and TAA-N/DON ratio (dots, right scale). b) Distribution of total combined carbohydrates (TCHO, bars, left scale) and TCHO-C/DOC ratio (dots, right scale). At each station four data are presented, corresponding to, from left to right, SURF, DCM, LIW and MDW layers, respectively. At stations ST10, ST1 and ST2, DON data at MDW and LIW layers were not available

Figure S2. a, b, c: Non linear least squares regression fits of Michaelis-Menten kinetics plotted for incremental ranges of substrate concentrations from 0.25 corresponding to a 0.025-0.25 µM substrate concentration set to 50 corresponding to a 0.025-50µM substrate concentration set for a) LAP, b) βGLU and c) AP. Dots correspond to the field measurements. The dataset is the same as in Figure 3: (DCM at station FAST), d, e f : corresponding distribution of the V and Km parameters plotted according to the maximum concentration added.

Figure S3. Distribution of heterotrophic bacterial production (BP, a) and bacterial abundances (BA, b). At each station four data are presented, corresponding to, from left to right, SURF, DCM, LIW and MDW layers, respectively. BP data are not available for LIW layer at stations ST2 and ST4, and MDW layer at station FAST, ST2, ST4, ST6.

Figure S4. Distribution of ectoenzyme activity ratios AP/LAP (a) and LAP/βGLU (b). Ratios calculated using Vm data from the global model (Vm_{all}) or the model 1 (Vm_1).

Supprimé: [1]
Supprimé: [1],
Supprimé:
Supprimé: [2,3]
Supprimé: [1,4]
Supprimé: [5]
Supprimé: [1]
Supprimé: [1]
Supprimé:
Supprimé: [1]
Supprimé: [6]
Supprimé: [6,7]
Supprimé: [1]
Supprimé: a range of data concentrations including
Supprimé: ed new
Supprimé: (For example 0.25 is plotted for a 0.025-0.25 concentration set, and 25 plotted for a 0.025-25 concentrationset).
Supprimé: This is the same data set
Supprimé: o
Supprimé: ,
Supprimé: DCM layer
Supprimé: m,
Supprimé: calculated
Supprimé: different concentrations ranges
Supprimé: tested

Table S1. Average standard deviations and ranges of biogeochemical parameters, nitrates (NO3), nitrites (NO2), dissolved inorganic phosphate (DIP), total chlorophyll a (TChl a), dissolved organic carbon (DOC), dissolved organic nitrogen (DON), dissolved organic phosphorus (DOP), total combined amino acids (TAA), total combined carbohydrates (TCHO), at the four layers sampled.*LWCC technique, ** classical method. < ld: below detection limit, nd: not sampled.

		SURF	DCM	LIW	MDW
NO3	mean ± sd	0.013 ± 0.018	0.88 ± 0.59	7.38 ± 2.57	8.29 ± 1.30
µM	range	<ld – 0.056	0.27 – 1.75	2.5 – 9.7	4.94 – 9.15
NO2	mean ± sd	< ld	106 ± 76	10 ± 4	< ld
nM	range	< ld	<ld – 216	<ld – 15	< ld
DIP	mean ± sd	10 ± 4*	35 ± 30*	0.29 ± 0.13**	0.36 ± 0.07**
nM*, µM**	range	4 – 17	9 – 107	0.05 – 0.43	0.17 – 0.41
TChl a	mean ± sd	0.08 ± 0.04	0.54 ± 0.15	nd	nd
µg l^{-1}	range	0.06 – 0.19	0.31 – 0.82		
DOC	mean ± sd	71 ± 4	62 ± 3	51 ± 4	45± 3
µM	range	60 – 75	58 – 66	45 – 58	39 – 49
DON	mean ± sd	5.7 ± 1.8	5.1 ± 1.2	3.6 ± 0.3	3.2 ± 0.4
µM	range	4.4 – 10.4	3.5 – 7.4	3.1 – 4.0	2.5 – 3.4
DOP	mean ± sd	0.05 ± 0.03	0.05 ± 0.04	0.04 ± 0.01	0.04 ± 0.01
µM	range	0.01 – 0.09	ld – 0.12	0.02 – 0.05	0.03 – 0.05
TAA	mean ± sd	216 ± 43	206 ± 31	76 ± 23	52 ± 14
nM	range	156 – 315	164 – 253	38 – 115	35 – 80
TCHO	mean ± sd	595 ± 43	351 ± 73	219 ± 55	427 ± 315
nM	range	547 – 671	278 – 471	162 – 328	111 – 950

Supprimé:

Supprimé: Ld

Supprimé: -

Table S2. Summary of statistics in the 3 series of Michaelis-Menten non linear regression fits. (Model 1: range of substrate concentrations 0.025 – 1 µM, Model 50: range of concentrations 2.5 – 50 µM), global model (the entire range of concentration 0.025 – 50 µM) for the 3 ectoenzymes (leucine aminopeptidase: LAP, beta glucosidase: βGLU, and alkaline phosphatase: AP). n: number of significant fits, se%: percentage of standard error estimated as ratio of standard error to fitted values for Km and Vm data. Biphasic cases: number of significant biphasic systems based on the Fisher test at $p < 0.1$ (see methods) compared to the number of samples where applying this test was possible (i.e. when the 2 fits where significant for the same sample). Biphasic indicator: $(Vm_1/Km_1) / (Vm_{50}/Km_{50})$ ratio.

	variable	SURF	DCM	LIW	MDW	All data
LAP Model 1	n	10	10	10	10	40
	se% Vm_1	23%	14%	19%	16%	
	se% Km_1	47%	33%	54%	53%	
LAP Model 50	n	10	10	10	10	40
	se% Vm_{50}	16%	10%	16%	17%	
	se% Km_{50}	50%	38%	44%	40%	
LAP gobal model	n	10	10	10	10	40
	se% Vm_{all}	10%	7%	11%	12%	
	se% Km_{all}	33%	24%	31%	26%	
LAP biphasic cases		6/10	5/10	2/10	4/10	17/40
LAP range of biphasic indicator		4-12	3-31	8-25	11-19	
βGLU Model 1	n	10	10	0	0	20
	se% Vm_1	12%	12%			
	se% Km_1	29%	22%			
βGLU Model 50	n	10	10	0	0	20
	se% Vm_{50}	10%	8%			
	se% Km_{50}	64%	48%			
βGLU gobal model	n	10	10	0	0	20
	se% Vm_{all}	11%	9%			
	se% Km_{all}	30%	29%			
βGLU biphasic cases		9/10	9/10			18/20
βGLU range of biphasic indicator		10 - 173	6 - 160			
AP Model 1	n	10	10	10	9	39
	se% Vm_1	6%	7%	14%	15%	
	se% Km_1	20%	19%	32%	34%	
AP Model 50	n	6	9	5	5	25
	se% Vm_{50}	9%	6%	12%	17%	
	se% Km_{50}	43%	44%	45%	54%	
AP gobal model	n	10	10	10	9	39
	se% Vm_{all}	6%	6%	8%	11%	
	se% Km_{all}	29%	26%	27%	36%	
AP biphasic cases		6/6	6/9	4/5	2/4	18/24
AP range of biphasic indicator		5 - 16	2 - 11	0.5 - 9	3 - 13	

Supprimé: ¶

Supprimé: 3

Tableau mis en forme

Tableau mis en forme

Tableau mis en forme

Supprimé: R

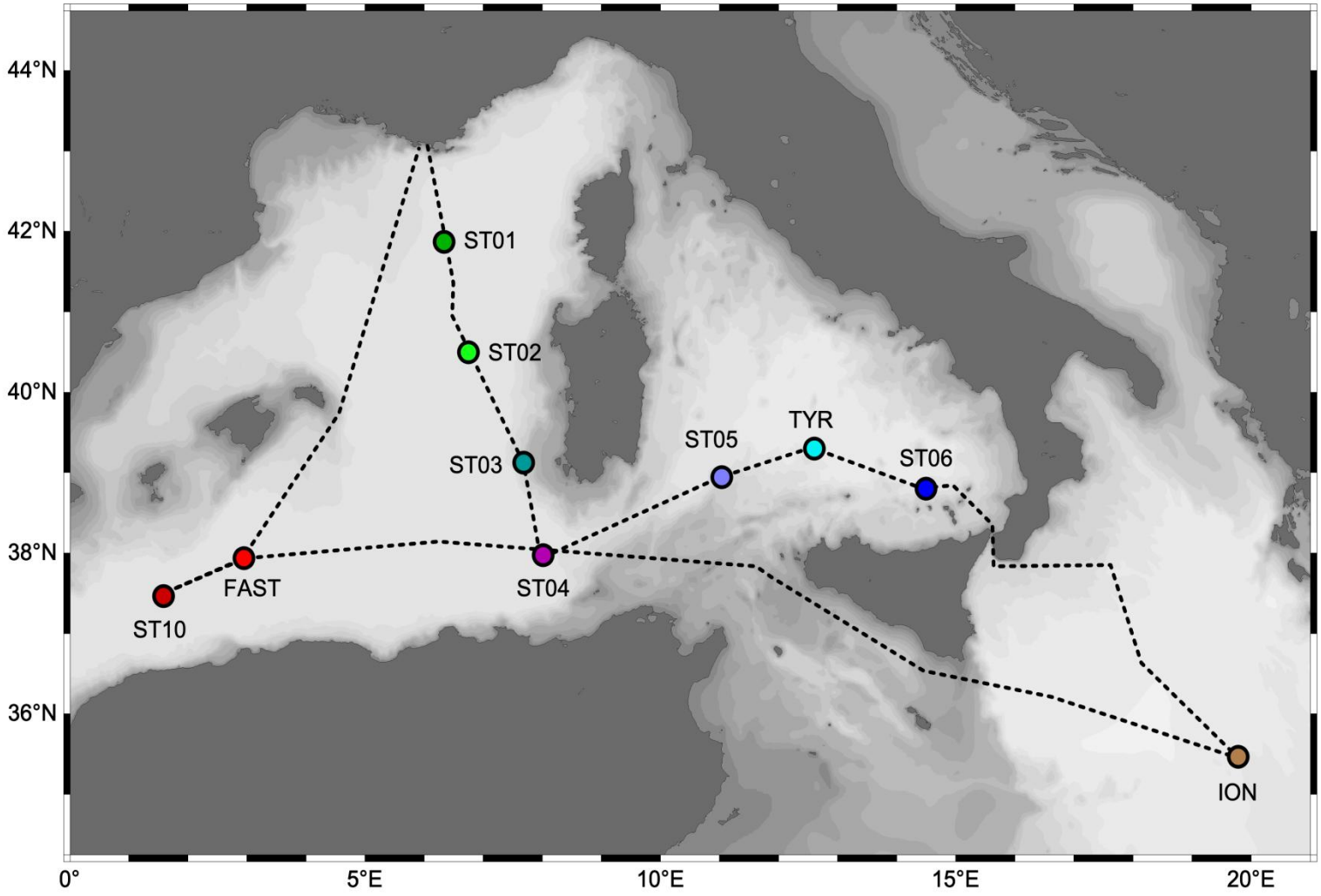
44°N
42°N
40°N
38°N
36°N
0°
5°E
10°E
15°E
20°E
ST01
ST02
ST03
ST04
ST05
TYR
ST06
FAST
ST10
ION

Fig 1

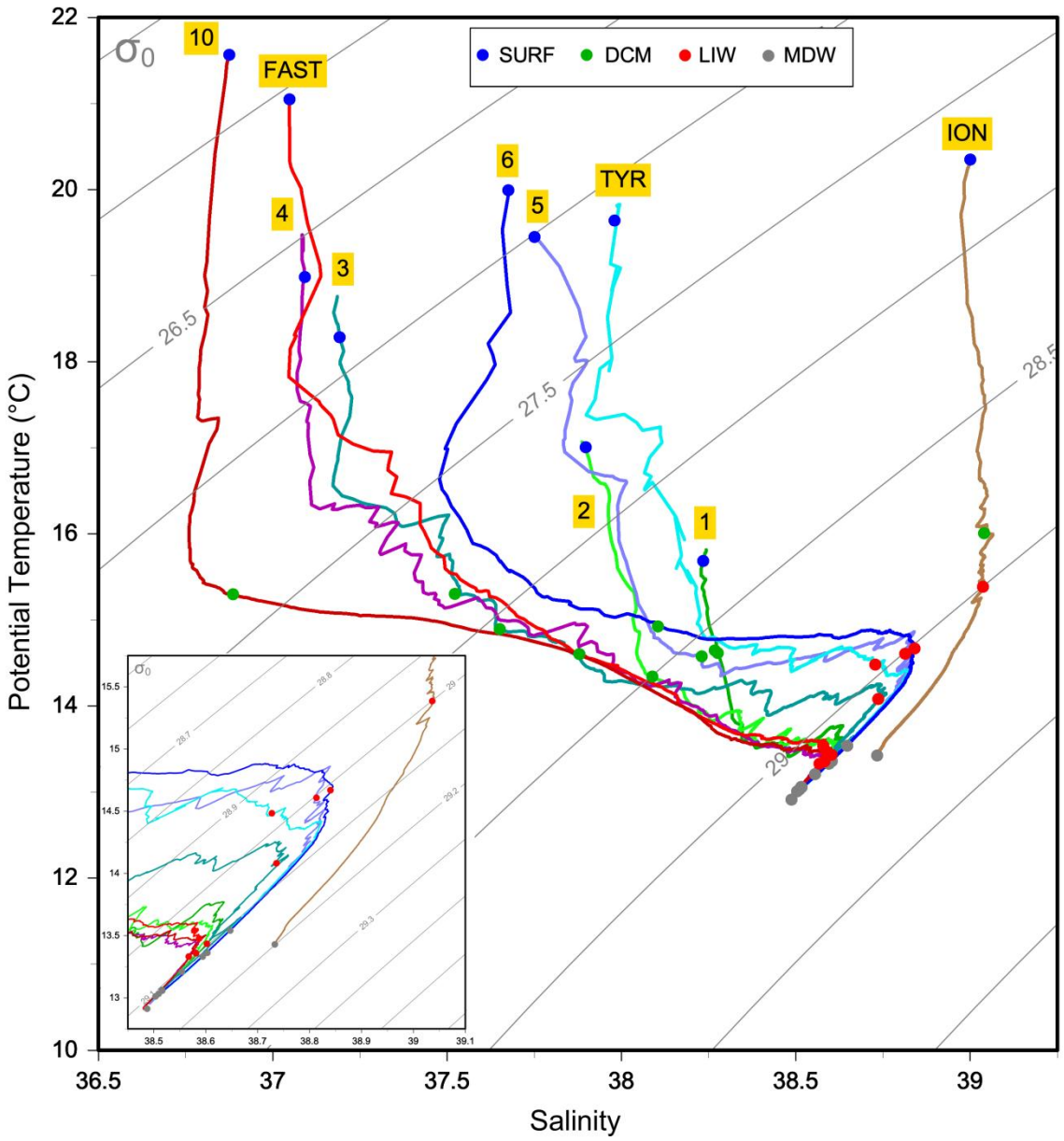
σ0
SURF
DCM
LIW
MDW
10
FAST
4
3
6
5
TYR
ION
2
1
26.5
27.5
28.5
29
Potential Temperature (°C)
Salinity
22
20
18
16
14
12
10
36.5
37
37.5
38
38.5
39

Fig 2

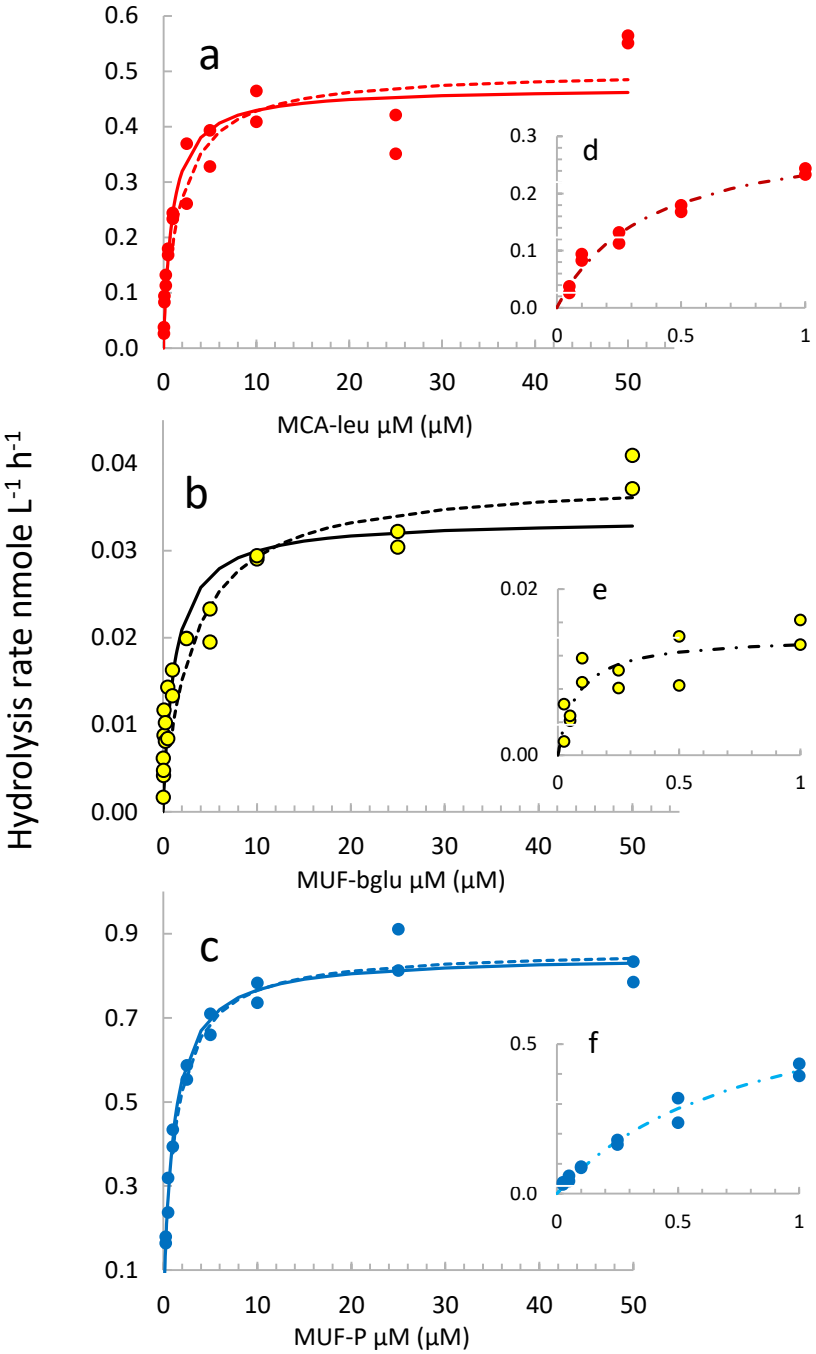
a
b
c
d
e
f
Hydrolysis rate nmole L-1 h-1
MCA-leu µM (µM)
MUF-bglu µM (µM)
MUF-P µM (µM)

Fig 3

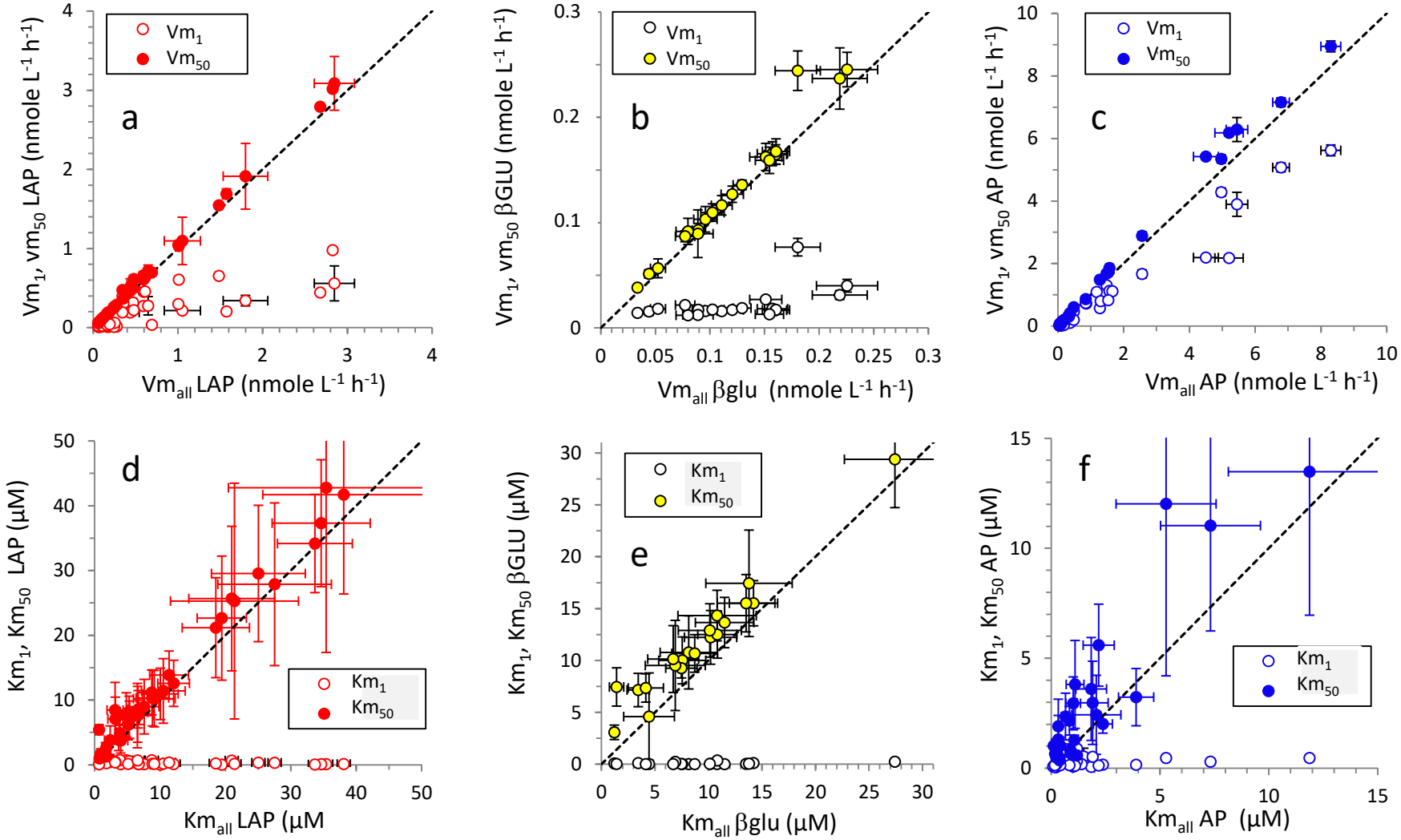
a
Vm1
Vm50
Vm1, vm50 LAP (nmole L-1 h-1)
Vmall LAP (nmole L-1 h-1)
b
Vm1
Vm50
Vm1, vm50 βGLU (nmole L-1 h-1)
Vmall βglu (nmole L-1 h-1)
c
Vm1
Vm50
Vm1, vm50 AP (nmole L-1 h-1)
Vmall AP (nmole L-1 h-1)
d
Km1
Km50
Km1, Km50 LAP (μM)
Kmall LAP (μM
e
Km1
Km50
Km1, Km50 βGLU (μM)
Kmall βglu (μM)
f
Km1
Km50
Km1, Km50 AP (μM)
Kmall AP (μM)

Fig 4

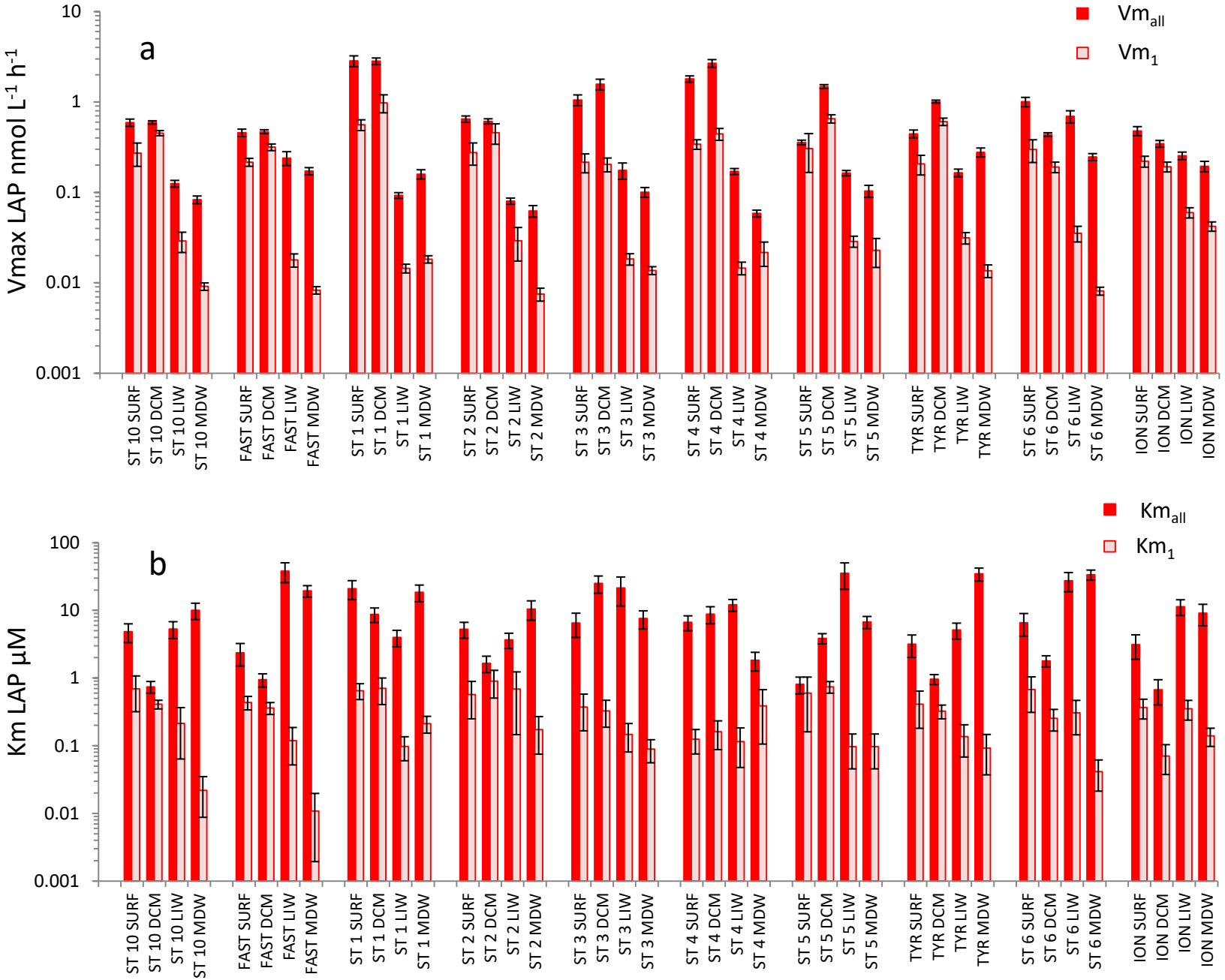
a
Vmax LAP nmol L-1 h-1
10
1
0.1
0.01
0.001
Vmall
Vm1
ST 10 SURF
ST 10 DCM
ST 10 LIW
ST 10 MDW
FAST SURF
FAST DCM
FAST LIW
FAST MDW
ST 1 SURF
ST 1 DCM
ST 1 LIW
ST 1 MDW
ST 2 SURF
ST 2 DCM
ST 2 LIW
ST 2 MDW
ST 3 SURF
ST 3 DCM
ST 3 LIW
ST 3 MDW
ST 4 SURF
ST 4 DCM
ST 4 LIW
ST 4 MDW
ST 5 SURF
ST 5 DCM
ST 5 LIW
ST 5 MDW
TYR SURF
TYR DCM
TYR LIW
TYR MDW
ST 6 SURF
ST 6 DCM
ST 6 LIW
ST 6 MDW
ION SURF
ION DCM
ION LIW
ION MDW
b
Km LAP µM
100
10
1
0.1
0.01
0.001
Kmall
Km1
ST 10 SURF
ST 10 DCM
ST 10 LIW
ST 10 MDW
FAST SURF
FAST DCM
FAST LIW
FAST MDW
ST 1 SURF
ST 1 DCM
ST 1 LIW
ST 1 MDW
ST 2 SURF
ST 2 DCM
ST 2 LIW
ST 2 MDW
ST 3 SURF
ST 3 DCM
ST 3 LIW
ST 3 MDW
ST 4 SURF
ST 4 DCM
ST 4 LIW
ST 4 MDW
ST 5 SURF
ST 5 DCM
ST 5 LIW
ST 5 MDW
TYR SURF
TYR DCM
TYR LIW
TYR MDW
ST 6 SURF
ST 6 DCM
ST 6 LIW
ST 6 MDW
ION SURF
ION DCM
ION LIW
ION MDW

Fig 5

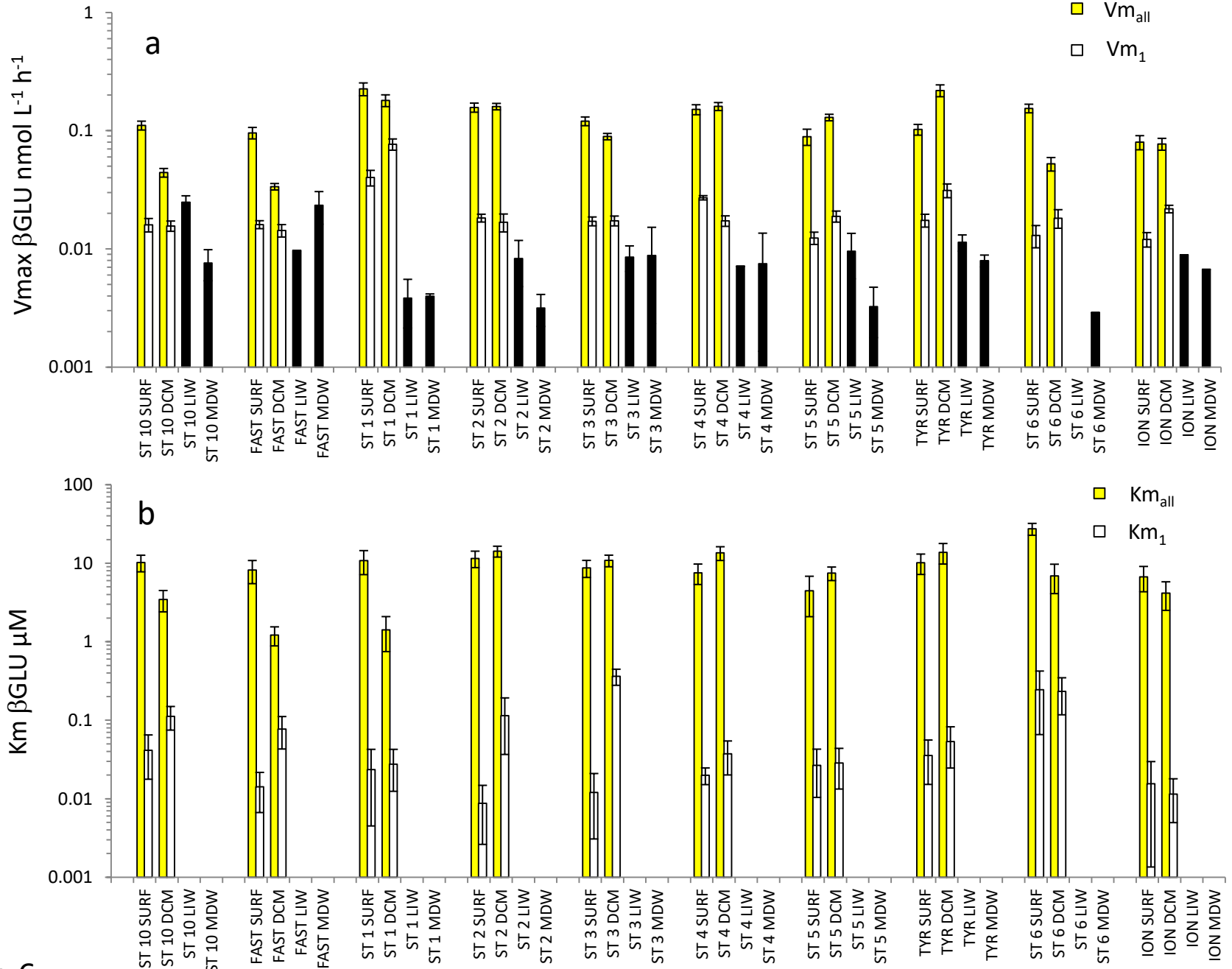
a
Vmax βGLU nmol L-1 h-1
1
0.1
0.01
0.001
Vmall
Vm1
b
Km βGLU µM
100
10
1
0.1
0.01
0.001
Kmall
Km1
ST 10 SURF
ST 10 DCM
ST 10 LIW
ST 10 MDW
FAST SURF
FAST DCM
FAST LIW
FAST MDW
ST 1 SURF
ST 1 DCM
ST 1 LIW
ST 1 MDW
ST 2 SURF
ST 2 DCM
ST 2 LIW
ST 2 MDW
ST 3 SURF
ST 3 DCM
ST 3 LIW
ST 3 MDW
ST 4 SURF
ST 4 DCM
ST 4 LIW
ST 4 MDW
ST 5 SURF
ST 5 DCM
ST 5 LIW
ST 5 MDW
TYR SURF
TYR DCM
TYR LIW
TYR MDW
ST 6 SURF
ST 6 DCM
ST 6 LIW
ST 6 MDW
ION SURF
ION DCM
ION LIW
ION MDW

Fig 6

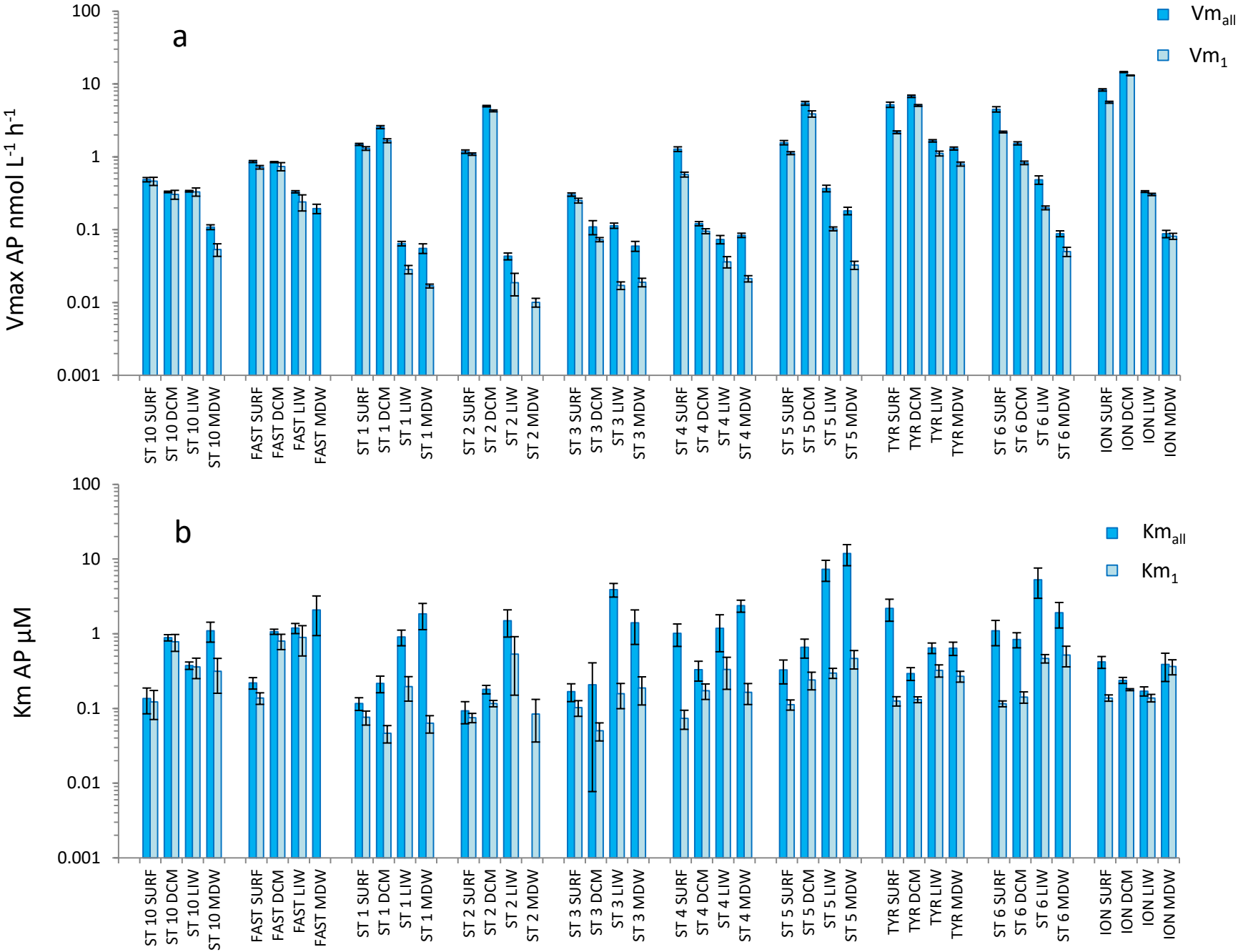
a
Vmax AP nmol L-1 h-1
100
10
1
0.1
0.01
0.001
Vmall
Vm1
ST 10 SURF
ST 10 DCM
ST 10 LIW
ST 10 MDW
FAST SURF
FAST DCM
FAST LIW
FAST MDW
ST 1 SURF
ST 1 DCM
ST 1 LIW
ST 1 MDW
ST 2 SURF
ST 2 DCM
ST 2 LIW
ST 2 MDW
ST 3 SURF
ST 3 DCM
ST 3 LIW
ST 3 MDW
ST 4 SURF
ST 4 DCM
ST 4 LIW
ST 4 MDW
ST 5 SURF
ST 5 DCM
ST 5 LIW
ST 5 MDW
TYR SURF
TYR DCM
TYR LIW
TYR MDW
ST 6 SURF
ST 6 DCM
ST 6 LIW
ST 6 MDW
ION SURF
ION DCM
ION LIW
ION MDW
b
Km AP µM
100
10
1
0.1
0.01
0.001
Kmall
Km1

Fig 7

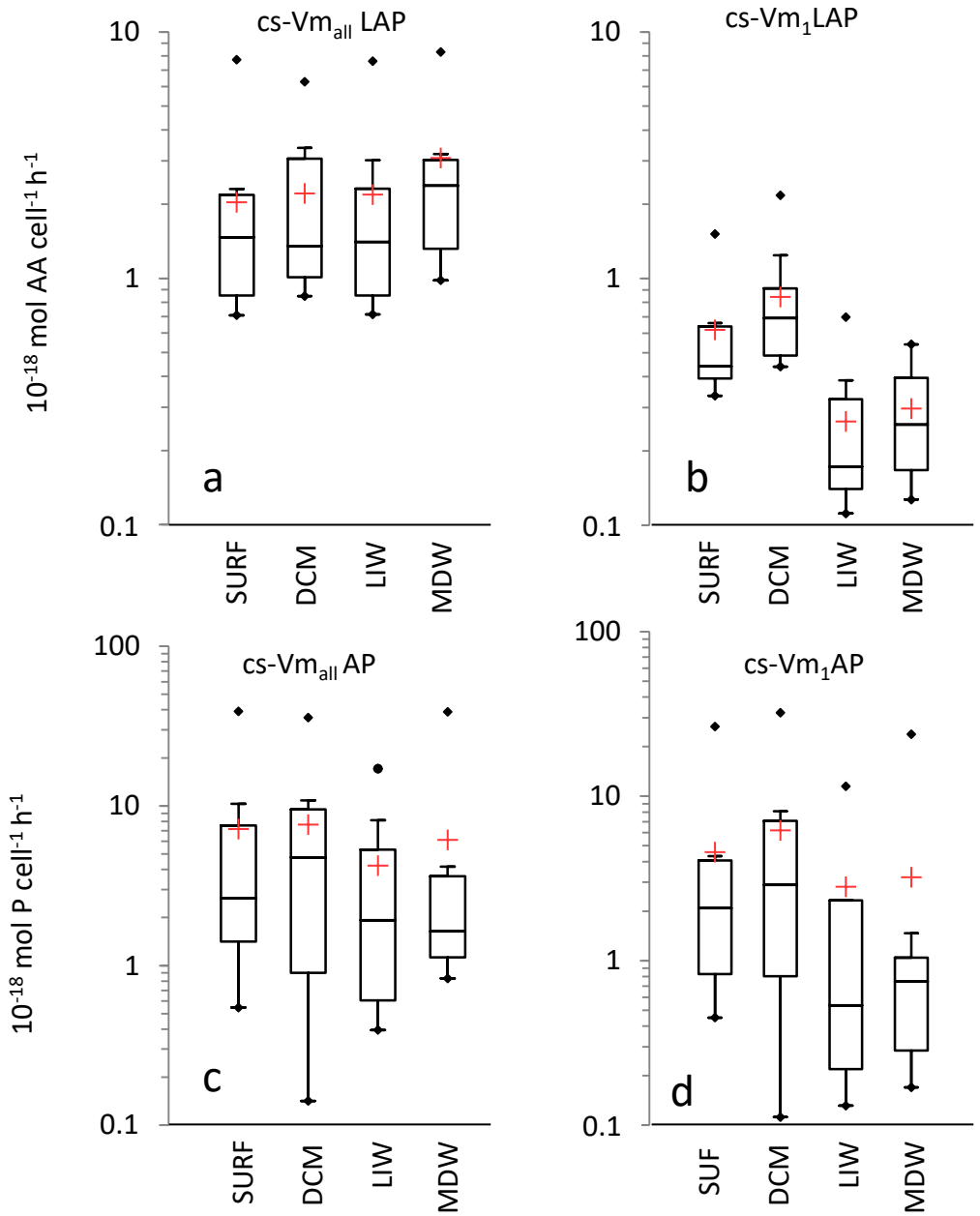
cs-Vm$_{all}$ LAP
cs-Vm$_1$LAP
cs-Vm$_{all}$ AP
cs-Vm$_1$AP
10^{-18} mol AA cell^{-1} h^{-1}
10^{-18} mol P cell^{-1} h^{-1}
10
1
0.1
100
a
b
c
d
SURF
DCM
LIW
MDW
SUF

Fig 8

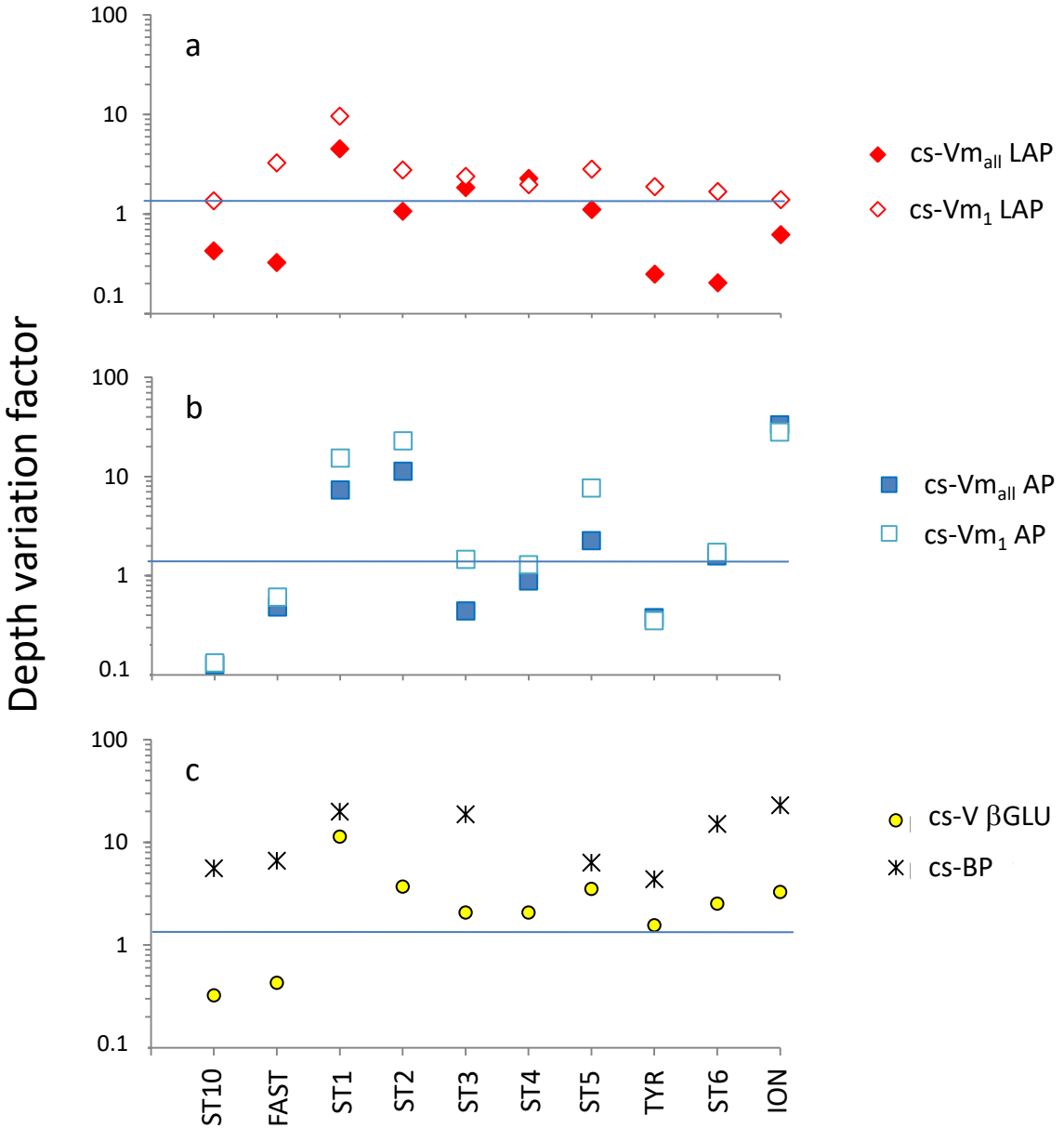
Depth variation factor
100
10
1
0.1
a
b
c
cs-Vm$_{all}$ LAP
cs-Vm$_1$ LAP
cs-Vm$_{all}$ AP
cs-Vm$_1$ AP
cs-V βGLU
cs-BP
ST10
FAST
ST1
ST2
ST3
ST4
ST5
TYR
ST6
ION

Fig 9

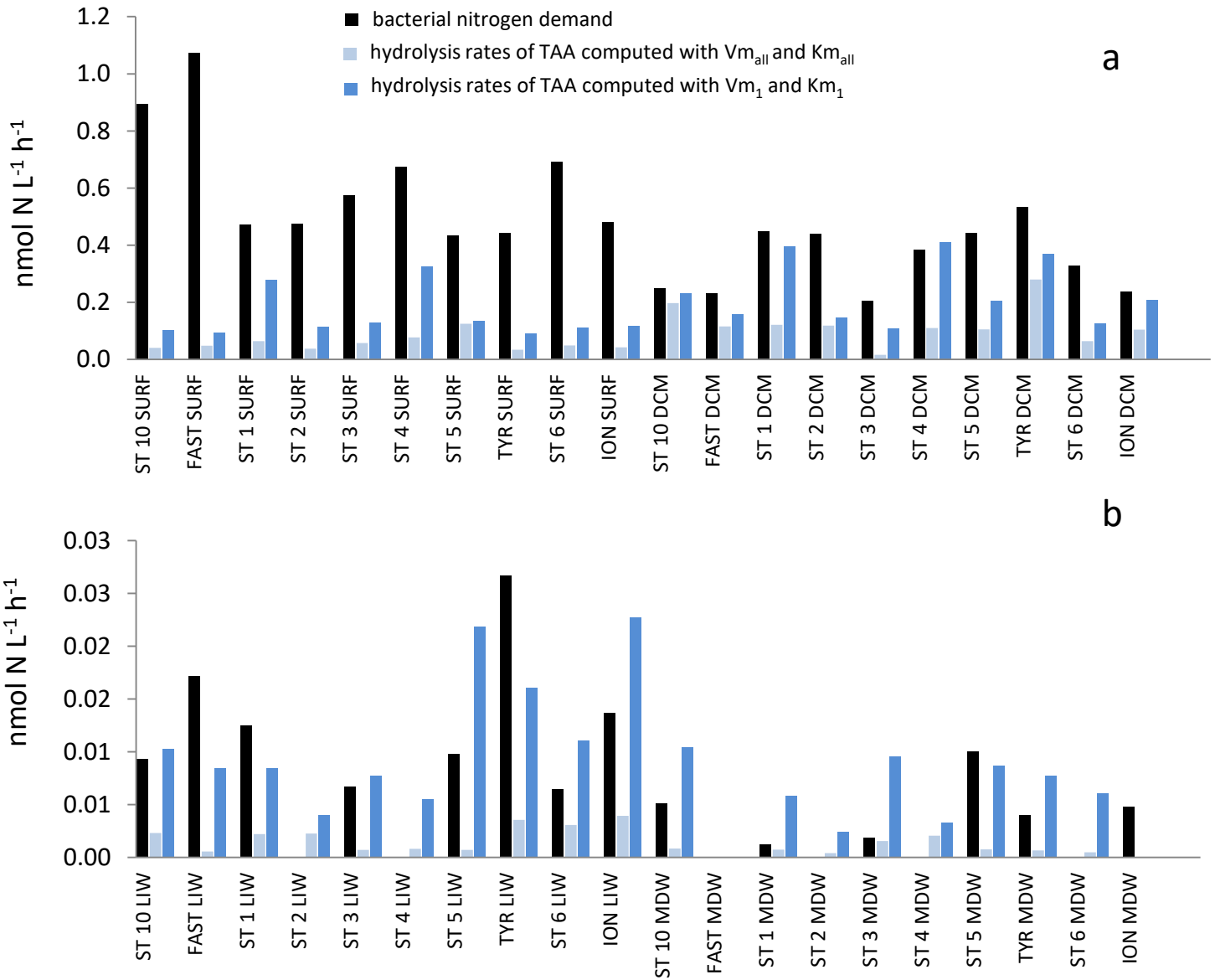
a
bacterial nitrogen demand
hydrolysis rates of TAA computed with Vm$_{all}$ and Km$_{all}$
hydrolysis rates of TAA computed with Vm$_1$ and Km$_1$
nmol N L^{-1} h^{-1}
1.2
1.0
0.8
0.6
0.4
0.2
0.0
ST 10 SURF
FAST SURF
ST 1 SURF
ST 2 SURF
ST 3 SURF
ST 4 SURF
ST 5 SURF
TYR SURF
ST 6 SURF
ION SURF
ST 10 DCM
FAST DCM
ST 1 DCM
ST 2 DCM
ST 3 DCM
ST 4 DCM
ST 5 DCM
TYR DCM
ST 6 DCM
ION DCM
b
nmol N L^{-1} h^{-1}
0.03
0.03
0.02
0.02
0.01
0.01
0.00
ST 10 LIW
FAST LIW
ST 1 LIW
ST 2 LIW
ST 3 LIW
ST 4 LIW
ST 5 LIW
TYR LIW
ST 6 LIW
ION LIW
ST 10 MDW
FAST MDW
ST 1 MDW
ST 2 MDW
ST 3 MDW
ST 4 MDW
ST 5 MDW
TYR MDW
ST 6 MDW
ION MDW

Fig 10

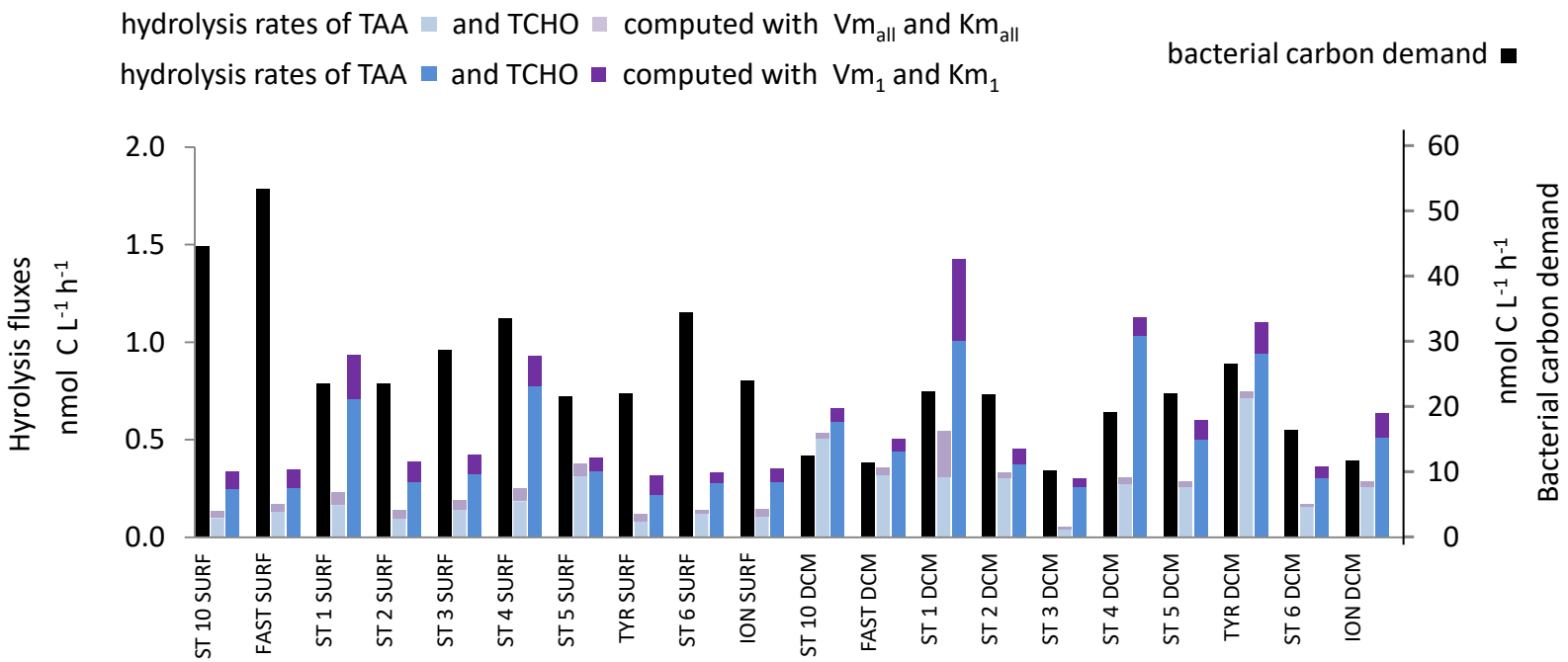
hydrolysis rates of TAA and TCHO computed with Vm$_{all}$ and Km$_{all}$
hydrolysis rates of TAA and TCHO computed with Vm$_1$ and Km$_1$
bacterial carbon demand
Hyrolysis fluxes nmol C L^{-1} h^{-1}
Bacterial carbon demand nmol C L^{-1} h^{-1}
2.0
1.5
1.0
0.5
0.0
60
50
40
30
20
10
0
ST 10 SURF
FAST SURF
ST 1 SURF
ST 2 SURF
ST 3 SURF
ST 4 SURF
ST 5 SURF
TYR SURF
ST 6 SURF
ION SURF
ST 10 DCM
FAST DCM
ST 1 DCM
ST 2 DCM
ST 3 DCM
ST 4 DCM
ST 5 DCM
TYR DCM
ST 6 DCM
ION DCM

Fig 11

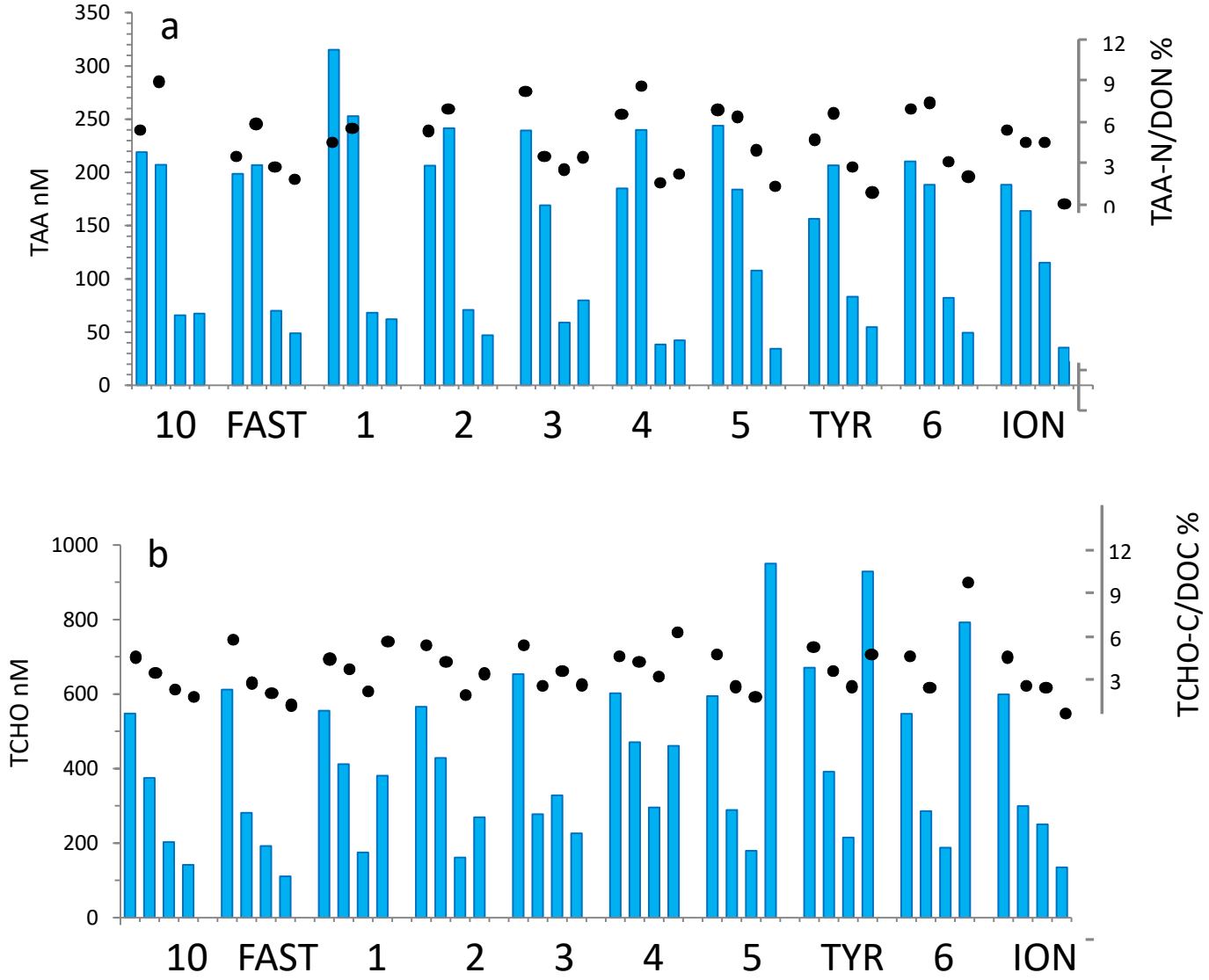
a
TAA nM
TAA-N/DON %
350
300
250
200
150
100
50
0
12
9
6
3
0
10
FAST
1
2
3
4
5
TYR
6
ION
b
TCHO nM
TCHO-C/DOC %
1000
800
600
400
200
0
12
9
6
3
10
FAST
1
2
3
4
5
TYR
6
ION

Fig S1

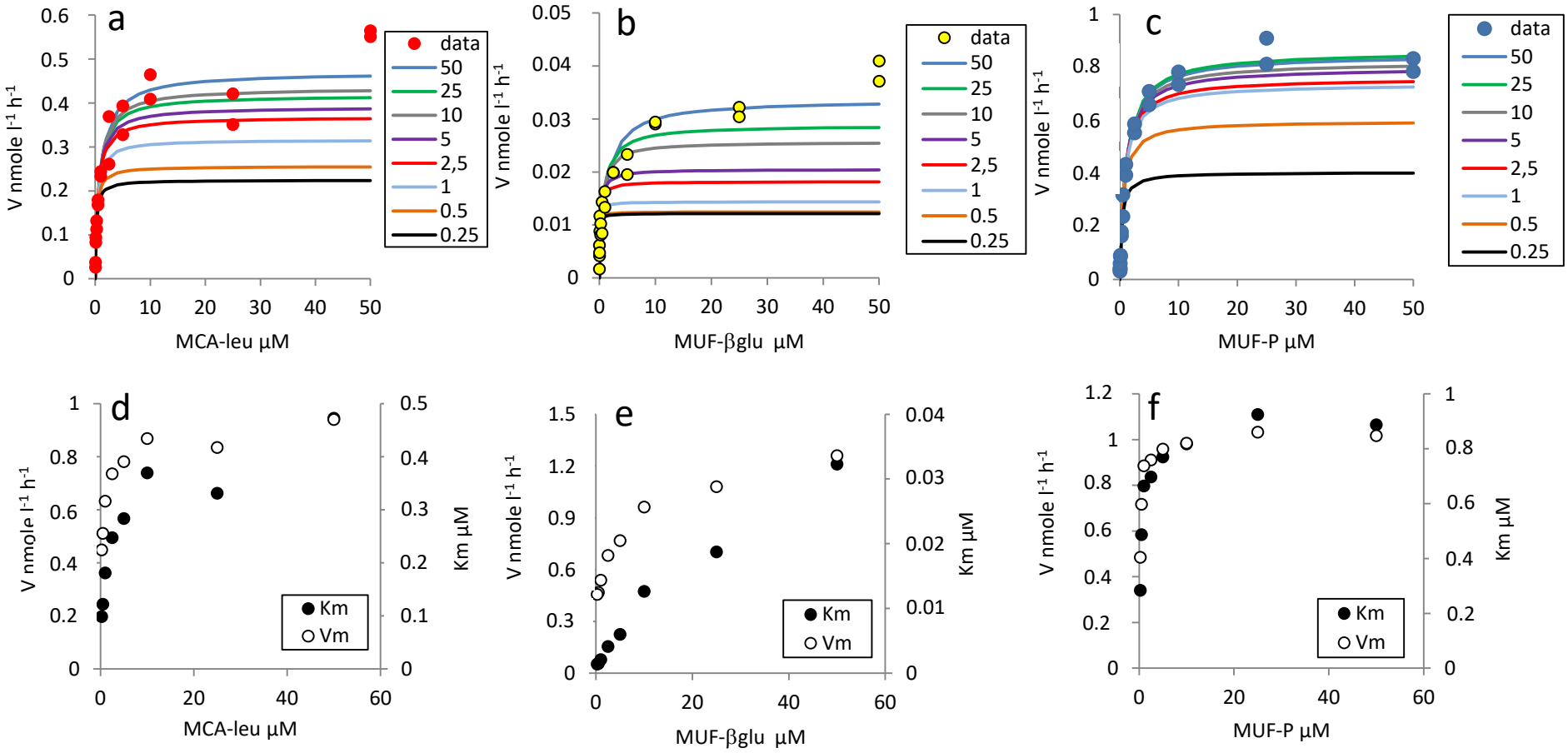
a
V nmole l-1 h-1
MCA-leu µM
data
50
25
10
5
2,5
1
0.5
0.25
b
V nmole l-1 h-1
MUF-βglu µM
c
V nmole l-1 h-1
MUF-P µM
d
V nmole l-1 h-1
Km µM
MCA-leu µM
Km
Vm
e
MUF-βglu µM
f
MUF-P µM

Fig S2

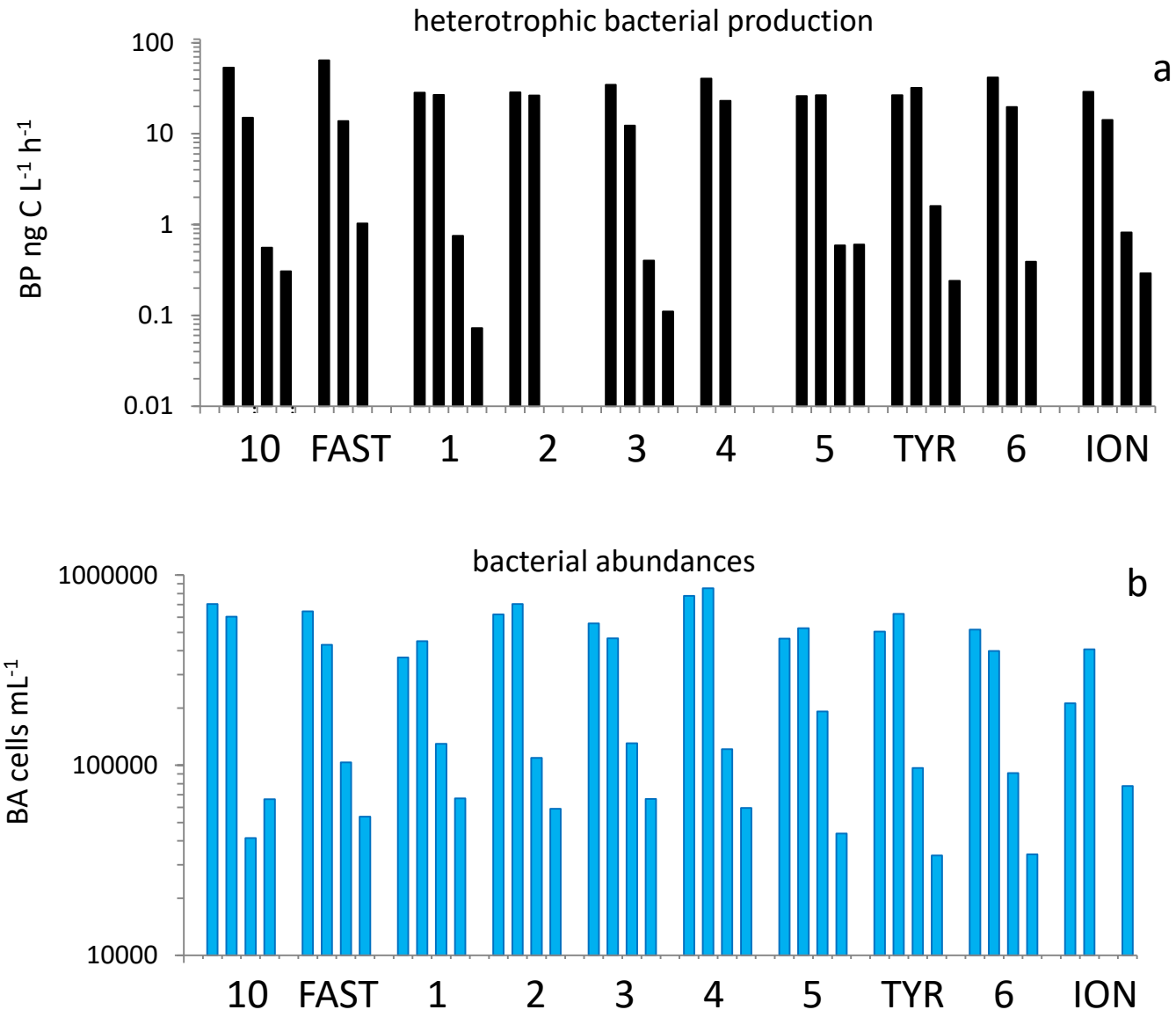
heterotrophic bacterial production
a
BP ng C L-1 h-1
100
10
1
0.1
0.01
10
FAST
1
2
3
4
5
TYR
6
ION
bacterial abundances
b
BA cells mL-1
1000000
100000
10000
10
FAST
1
2
3
4
5
TYR
6
ION

Fig S3

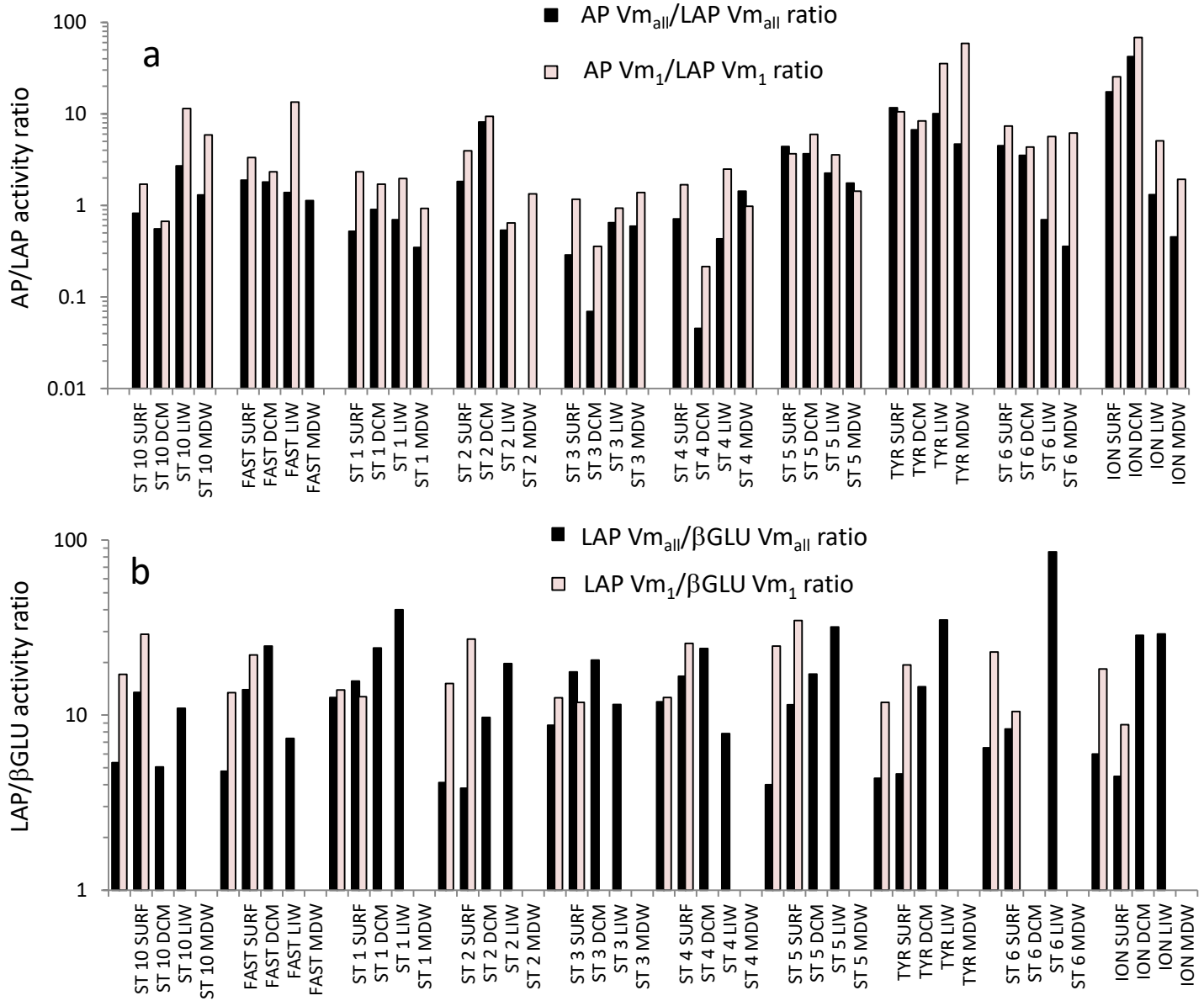
a
AP Vm$_{all}$/LAP Vm$_{all}$ ratio
AP Vm$_1$/LAP Vm$_1$ ratio
AP/LAP activity ratio
100
10
1
0.1
0.01
b
LAP Vm$_{all}$/βGLU Vm$_{all}$ ratio
LAP Vm$_1$/βGLU Vm$_1$ ratio
LAP/βGLU activity ratio
100
10
1
ST 10 SURF
ST 10 DCM
ST 10 LIW
ST 10 MDW
FAST SURF
FAST DCM
FAST LIW
FAST MDW
ST 1 SURF
ST 1 DCM
ST 1 LIW
ST 1 MDW
ST 2 SURF
ST 2 DCM
ST 2 LIW
ST 2 MDW
ST 3 SURF
ST 3 DCM
ST 3 LIW
ST 3 MDW
ST 4 SURF
ST 4 DCM
ST 4 LIW
ST 4 MDW
ST 5 SURF
ST 5 DCM
ST 5 LIW
ST 5 MDW
TYR SURF
TYR DCM
TYR LIW
TYR MDW
ST 6 SURF
ST 6 DCM
ST 6 LIW
ST 6 MDW
ION SURF
ION DCM
ION LIW
ION MDW

Fig S4